

NASA TM X-620

(NASA-TM-X-620) WIND TUNNEL INVESTIGATION
OF A SUPERSONIC FAN-IN-FUSELAGE VTOL
FIGHTER MODEL AT ZERO AND LOW FORWARD
SPEEDS (NASA) 45 p

62 72444 Copy 4
NASA TM X-620
N73-74547
Unclas
00/99 19235





X67-86062

TECHNICAL MEMORANDUM

CLASSIFICATION CHANGE

TO -
X-620

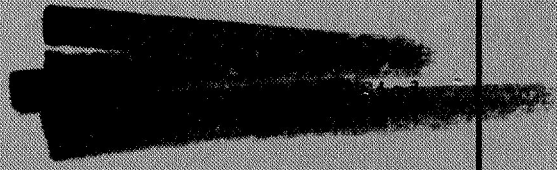
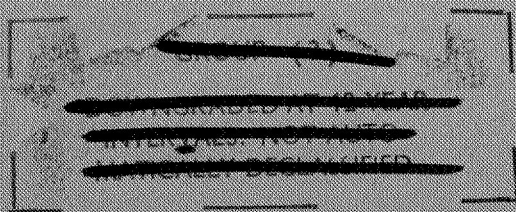
UNCLASSIFIED

By authority of  No. 73-378
Changed by  Date 6/7/72

WIND-TUNNEL INVESTIGATION OF A SUPERSONIC FAN-IN-FUSELAGE VTOL FIGHTER MODEL AT ZERO AND LOW FORWARD SPEEDS

By Kenneth P. Spreemann

Langley Research Center
Langley Station, Hampton, Va.

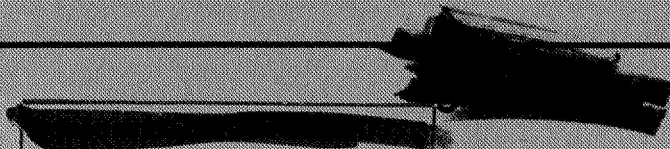


CLASSIFIED DOCUMENT - TITLE CONFIDENTIAL

This material contains information affecting the National Defense of the United States within the meaning of the espionage laws, Title 18, U.S.C., Secs. 793 and 794, the transmission or revelation of which in any manner to an unauthorized person is prohibited by law.

NATIONAL AERONAUTICS AND SPACE ADMINISTRATION
WASHINGTON

June 1962



Available from NASA to U. S.
Government and U. S.
Government contractors only.

M

Upgraded to Confidential by
authoritative Classification Change
Notes No. 113 Date 6/28/67

~~CONFIDENTIAL~~

NATIONAL AERONAUTICS AND SPACE ADMINISTRATION

TECHNICAL MEMORANDUM X-620

WIND-TUNNEL INVESTIGATION OF A
SUPERSONIC FAN-IN-FUSELAGE VTOL FIGHTER MODEL

AT ZERO AND LOW FORWARD SPEEDS*

By Kenneth P. Spreemann

SUMMARY

~~NOFORN~~

An investigation of a 1/10-scale model of a proposed supersonic fan-in-fuselage fighter has been conducted in the Langley 300-MPH 7-by 10-foot tunnel at zero and low forward speeds. The model has three ducted fans in tandem which are used for vertical take-off and landing. Sets of louvers under the fans deflect the fan stream rearward to provide the thrust required for transition from hovering to forward flight.

In the static or hovering condition a sizable loss in lift and a nose-up pitching moment were encountered in ground effect. For these same conditions either a large fence on the fuselage lower surface or the landing gear with doors reduced the losses in lift and the nose-up pitching moments encountered by the clean model very close to the ground. However, at intermediate heights these modifications were ineffective.

The forward-speed data, all of which were run out of ground effect, showed that the model experienced large losses in lift and large nose-up pitching moments at low angles of attack in the transition speed range. By going to higher angles of attack the losses in total lift could be partially reduced. However, the nose-up pitching moments were increased by going to higher angles of attack. None of the fences or modifications tried on the model alleviated the nose-up tendencies.

INTRODUCTION

In the past few years considerable attention has been directed toward a VTOL system in which fans are buried horizontally in the wing or fuselage. These fans are driven by turbojet engines whose exhaust gases are directed through a turbine mounted at the periphery of the

*Title, Confidential.

~~CONFIDENTIAL~~
Released from NASA to U. S.
Government and U. S.
Government contractors

~~CONFIDENTIAL~~

fans. By this system static lifts two to four times the thrust of the propulsion engines can be obtained. In transition from hovering to forward flight the fan streams are gradually deflected rearward to provide acceleration. When sufficient speed has been obtained for aerodynamic lift to support the aircraft the fans are cut off and closed over, and the airplane is flown as a conventional turbojet aircraft. This concept has given rise to a new family of high-performance airplanes presently termed fan-in-fuselage or fan-in-wing VTOL configurations.

An investigation of a model of such a configuration, a proposed supersonic fan-in-fuselage VTOL fighter, to determine the aerodynamic characteristics at zero and low forward speeds has been conducted in the Langley 300-MPH 7- by 10-foot tunnel. A dynamically scaled model of this configuration has also been tested in the Langley full-scale tunnel, and these results are reported in reference 1. The model has three lift fans in tandem buried in the fuselage which are used for vertical take-off and landing. Sets of louvers under the fans deflect the fan streams rearward to provide the thrust required to perform the transition to forward flight.

L
1
7
4
8

SYMBOLS

The positive senses of forces, moments, and angles are indicated in figure 1(a) for the static tests and in figure 1(b) for the wind-tunnel tests. The pitching moments are referred to the 0.396 point of the mean aerodynamic chord unless otherwise noted.

b	wing span, ft
c	local wing chord, ft
\bar{c}	mean aerodynamic chord, $\frac{2}{S} \int_0^{b/2} c^2 dy$, ft
C_L	lift coefficient, L/qS
C_m	pitching-moment coefficient, $M/qS\bar{c}$
C_X	longitudinal-force coefficient, F_X/qS
D	fan diameter, ft
F	resultant force from tunnel tests, lb
F'	resultant force from static tests, lb

~~CONFIDENTIAL~~

~~CONFIDENTIAL~~

L
1
7
4
8

- F'_{∞} resultant force from static tests out of ground effect without modifications or landing gear (equals T_0 for $\delta = 90^\circ$), lb
- F_X longitudinal force from tunnel tests, Thrust - Drag, lb
- F'_X longitudinal force from static tests, lb
- ΔF_X increment in longitudinal force due to interference, lb
- h height of moment reference center above ground board, ft
- L lift from tunnel tests, lb
- L' lift from static tests, lb
- ΔL increment in lift due to interference, lb
- l_g height of landing gear (measured from bottom of fuselage), 0.506 ft
- M pitching moment from tunnel tests, ft-lb
- M' pitching moment from static tests, ft-lb
- ΔM increment in pitching moment due to interference, ft-lb
- n number of fans
- q free-stream dynamic pressure, $\frac{1}{2}\rho V_{\infty}^2$, lb/sq ft
- N fan speed, rpm
- R Reynolds number, $\frac{\rho V_{\infty} \bar{c}}{\mu}$
- S reference wing area, 6.0 sq ft
- T_0 static thrust of fans out of ground effect with $\delta = 90^\circ$, lb
- V_{∞} free-stream velocity, ft/sec
- V_j velocity in fan slipstream, $\sqrt{\frac{T_0}{\rho_s n \pi \frac{D^2}{4}}}$, ft/sec
- y spanwise distance, ft

~~CONFIDENTIAL~~

4

~~CONFIDENTIAL~~

z distance from moment reference center to exit louvers (bottom of fuselage), ft
 α angle of attack, tunnel data, deg
 γ model attitude angle, static data, deg
 δ louvers angle with respect to fuselage reference plane, deg
 δ_e elevator deflection with respect to fuselage reference plane, deg
 θ static turning angle (inclination of resultant force vector measured from longitudinal-force axis), $\tan^{-1} \frac{L'}{F_X}$, deg
 ρ mass density of air in free stream, slugs/cu ft
 ρ_s mass density of air in fan slipstream, slugs/cu ft
 μ coefficient of viscosity, lb-sec/sq ft

Subscripts:

1 power on
 2 power off

L
1
7
4
8

MODEL AND APPARATUS

A drawing of the 1/10-scale model with pertinent dimensions is presented in figure 2. Two photographic views of the model are presented in figure 3. The 1/16-inch-diameter cables restraining the model from diverging under load, also shown in figure 3, were attached to the top and bottom balance turntables and were therefore an integral part of the whole model and balance system. The air loads on the cables were estimated to be about 10 percent of the power-off drag of the clean model.

The model had a conically cambered 63.5° delta wing of aspect ratio 2.1. Details of the main landing gear are given in figure 4. Diagrams of the fences and modifications employed on the model are shown in figures 5 to 8.

The model represents a configuration which has three lift fans buried in the fuselage powered by the exhaust gases of six turbojet engines. Each of the four-bladed fans in the model was driven by a

~~CONFIDENTIAL~~

~~CONFIDENTIAL~~

5

compressed air jet at the tip of each blade. Louvers under the three lift fans were used to deflect the fan streams rearward to provide the thrust required to perform the transition from hovering to forward flight. These louvers had adjustments from 90° (vertical with respect to the fuselage reference plane) to 60° rearward in 10° increments. In this model the jet inlets were faired over, thus precluding simulation of jet flow through the model.

TESTS AND CORRECTIONS

The static tests were conducted in a large room in the Langley 7-by 10-Foot Tunnels Branch. The tunnel tests were made in the Langley 300-MPH 7-by 10-foot tunnel.

Fan speed was controlled by means of individual valves in the lines leading to each fan, thus enabling the operator to match speeds in all the fans for the static or hovering condition. Since it was impractical to adjust fan speeds for each angle of attack in the tunnel tests, the fan speeds were matched at zero angle of attack with the tunnel set at the desired speed. This procedure allowed a variation from about 2 to -2 percent in fan speed throughout the angle-of-attack range.

The test Reynolds number, based on the wing mean aerodynamic chord and tunnel velocity, varied from 0.49×10^6 to 2.0×10^6 . It is believed that some tunnel-wall effects are present in the data because the static thrust measured in the tunnel was about 5 to 8 percent lower than that measured in the static room. The magnitude of the tunnel-wall interference effects was not determined. It is believed that these effects would be largely reduced with greater ratios of tunnel size to model size. The static thrust measured in the tunnel was used in reducing the tunnel data and the static thrust measured in the static room was used in reducing the static data. Blockage and jet-boundary corrections were not applied to the data since little had been done to provide tunnel corrections for powered models of this type prior to this investigation. However, some insight into these corrections is available in a recently published paper (ref. 2). Application of these tunnel corrections would, in general, raise the level of the model lift. However, the incremental data for the various configurations are believed to be valid.

PRESENTATION OF RESULTS

The results of the investigation are presented in the following figures:

~~CONFIDENTIAL~~

~~CONFIDENTIAL~~

	Figure
Static data:	
Fan calibration	9
Effect of height above ground for various model conditions . .	10, 11
Effect of louvers angle	12
Forward-speed data:	
Power-off characteristics	13 to 15
Power-on:	
Basic aerodynamic characteristics -	
$\delta = 90^\circ$	16
$\delta = 60^\circ$	17
Effect of various fences	18
Effect of various modifications	19
Summary data	20, 21

The basic data for the summary figures (figs. 20 and 21) were obtained from figures 16 and 17.

L
1
7
4
8

DISCUSSION

Static Data

Within ground effect sizable nose-up pitching moments and losses in lift were encountered by the clean model. (See fig. 10.) At intermediate ground heights, (about 2 to 4 landing-gear heights) a large streamwise fence on the lower surface of the fuselage or landing gear, which had doors attached to it thus providing the equivalent of a fence, had little effect on the resultant force, pitching moment, or turning angle (fig. 10). However, very close to the ground (below 2 landing-gear heights) the nose-up pitching moments and losses in lift were reduced. The results of changes in model attitude given in figure 11 show that within ground effect losses in the ratio of lift to thrust L'/T_0 and increases in nose-up moments were experienced by the model with increases in attitude.

In figure 12 showing the effects of louvers angle of the midfan only, the moment reference center is at the center of the midfan rather than at 0.396c as is the case for all the other data.

Forward-Speed Data

The basic power-off longitudinal coefficients presented in figures 13 to 15 indicate that in the cruise condition (fan inlets and

~~CONFIDENTIAL~~

~~CONFIDENTIAL~~

7

exits sealed) the model is longitudinally unstable. Opening the fan inlets and exits causes an increase in drag, a reduction in lift-curve slope, and a rearward shift in the aerodynamic center (fig. 13).

Moving the wing rearward 9.3 percent \bar{c} reduced the longitudinal instability as shown in figure 14. All of the data (except that in fig. 14) were run with the wing in the forward position as shown in figure 2.

The basic power-on data shown in figures 16(b) and 17(b) indicate that large nose-up moments were encountered with increases in forward speed. This increase in nose-up moment was experienced on a dynamically scaled model flown in the Langley full-scale tunnel. (See ref. 1.) In the flight tests of that investigation the nose-up moments became so large that transition from hovering to full forward speed could not be accomplished. None of the fences or modifications tried on the model in the present investigation alleviated these nose-up pitching moments. (See figs. 18 and 19.)

The summary data in figure 20 more clearly demonstrate the adverse forward-speed effects on this particular configuration. These data show that large losses in lift at low angles of attack were encountered in the transition speed range, but by going to higher angles of attack the losses in total lift could be partially reduced. At these higher angles of attack, for L/T_0 greater than 1.0 this configuration is experiencing a large decelerating force ($-F_x/T_0$). Also, the nose-up pitching moments increased with forward velocity and were further aggravated by going to higher angles of attack (fig. 20).

A detailed discussion of the basic source of these positive pitching moments and losses in lift is given in reference 3 covering an investigation of a deflected jet model at zero and low forward speeds. Briefly, what has been found is that on the lower surface positive pressures were generated in front of the jet or fan stream and much larger negative pressures behind, thus inducing losses in lift and large nose-up pitching moments.

The increments in lift, longitudinal force, and pitching moment induced on the model by the effects of the fan streams (fig. 21) have been taken from the data of figures 17 and 18 by defining the total forces and moments on the model in terms of the components by the following expressions:

$$L_1 = F' \sin \theta + C_{L,2} q S + \Delta L$$

~~CONFIDENTIAL~~

~~CONFIDENTIAL~~

$$F_{X,1} = F' \cos \theta + C_{X,2} q S + \Delta F_X - T_0 \frac{V_\infty}{V_j}$$

$$M_1 = F' z \cos(\theta - \gamma) + C_{m,2} q S \bar{c} + \Delta M$$

The quantity on the left-hand side of the equal sign represents the total measured force or moment (fig. 20). The first quantity on the right-hand side of the equal sign is the direct thrust contribution, the second term is the aerodynamic force or moment as determined from the power-off data of figure 13, and the third term is the interference increment. The fourth term on the right-hand side of the longitudinal-force equation is the intake momentum drag. This term is not accounted for in the pitching-moment increment ΔM ; thus, the pitching-moment increment includes both the inlet and exit contributions. A theoretical treatment of the inlet contribution to the moment is presented in reference 4. In reducing the data the value of T_0 was substituted for F' in these equations.

The increments of lift, longitudinal force, and pitching moment due to jet interference are presented in figure 21 and are calculated from the following expressions which were derived from the basic equations previously given:

$$\frac{\Delta L}{T_0} = \frac{L_1}{T_0} - \left(\sin \theta + \frac{C_{L,2} q S}{T_0} \right)$$

$$\frac{\Delta F_X}{T_0} = \frac{F_{X,1}}{T_0} - \left(\cos \theta + \frac{C_{X,2} q S}{T_0} - \frac{V_\infty}{V_j} \right)$$

$$\frac{\Delta M}{T_0 \bar{c}} = \frac{M_1}{T_0 \bar{c}} - \left[\frac{z \cos(\theta - \gamma)}{\bar{c}} + \frac{C_{m,2} q S}{T_0} \right]$$

The results indicate that the interference effects on lift and pitching moment are in general a function of both forward velocity and angle of attack, whereas the deflected jet reported in reference 3 was principally affected by forward velocity. These interference effects become more severe with increases in angle of attack, which are shown as greater losses in lift and increases in nose-up pitching moments (fig. 21).

~~CONFIDENTIAL~~

~~CONFIDENTIAL~~

The decrement in lift-thrust ratio at zero velocity with the 60° louver angle as compared with that with the 90° louver angle (fig. 21) is due to the louver turning losses.

SUMMARY OF RESULTS

L An investigation of a model of a proposed supersonic fan-in-fuselage
1 VTOL fighter indicated that in the static or hovering condition the losses
7 in resultant force and the nose-up pitching moments encountered by the
4 clean model very close to the ground were reduced by the addition of a
8 large streamwise fence on the lower surface of the fuselage or by the
landing gear with doors attached. However, at intermediate heights these
modifications were ineffective.

The forward-speed data showed that the model experienced large losses in lift and large nose-up moments at low angles of attack in the transition from hovering to forward flight. By going to higher angles of attack the losses in total lift could be partially reduced. The nose-up pitching moments increased with forward velocity and were in general greater at higher angles of attack. None of the fences or modifications employed on the model alleviated these nose-up tendencies. The data indicated that the interference effects on lift and pitching moment are a function of both forward speed and angle of attack.

Langley Research Center,
National Aeronautics and Space Administration,
Langley Air Force Base, Va., October 10, 1961.

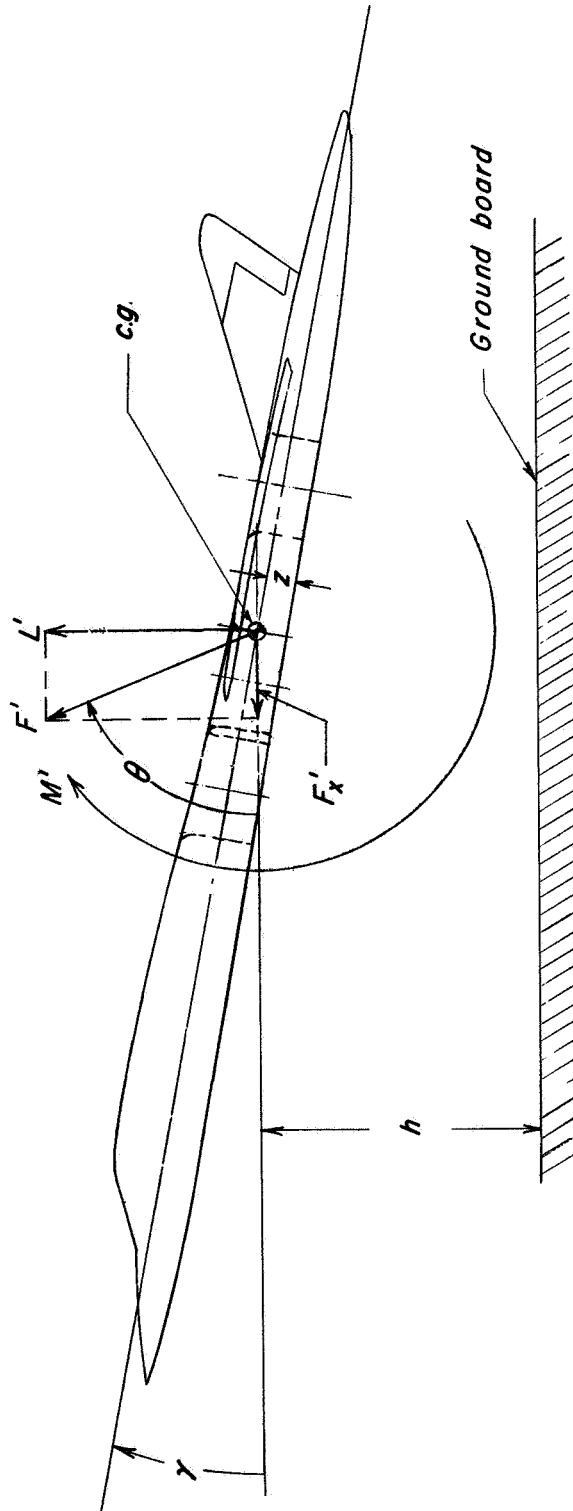
~~CONFIDENTIAL~~

~~CONFIDENTIAL~~

REFERENCES

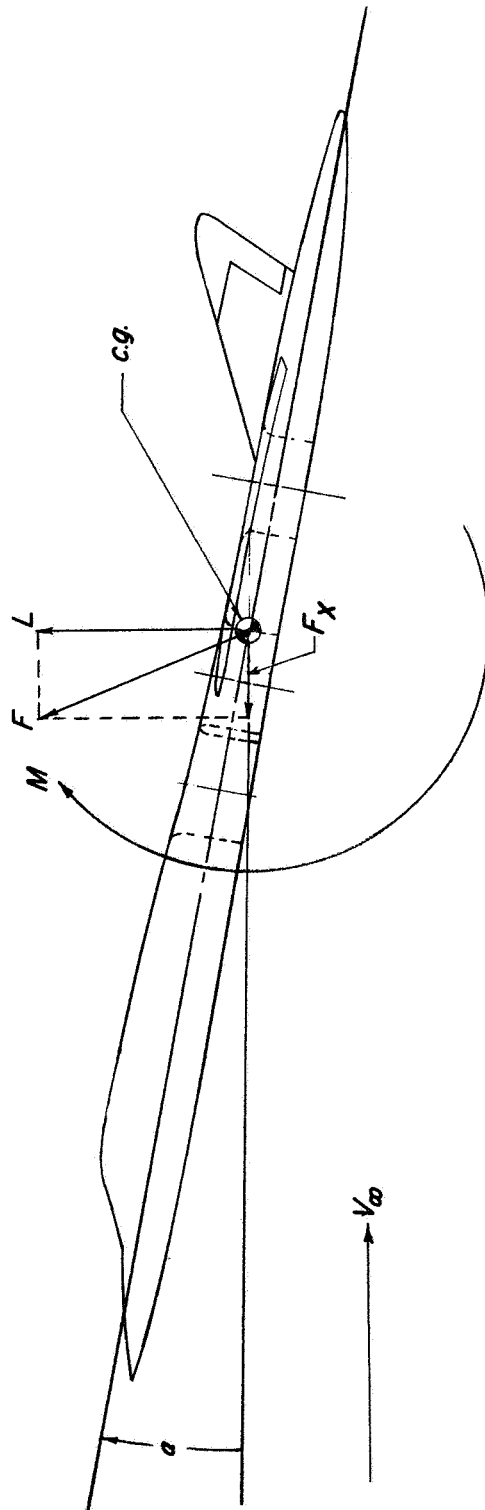
1. Kirby, Robert H.: Hovering and Transition Flight Test of a Supersonic Fan-In-Fuselage VTOL Fighter Model. NASA TM X-424, 1961.
2. Heyson, Harry H.: Linearized Theory of Wind-Tunnel Jet-Boundary Corrections and Ground Effect for VTOL-STOL Aircraft. NASA TR R-124, 1962.
3. Spreemann, Kenneth P.: Investigation of Interference of a Deflected Jet With Free Stream and Ground on Aerodynamic Characteristics of a Semispan Delta-Wing VTOL Model. NASA TN D-915, 1961.
4. Theodorsen, Th.: Theoretical Investigation of Ducted Propeller Aerodynamics. Vols. I and II, Contract No. DA 44-177-TC-606, Republic Aviation Corp., Aug. 10, 1960.

L
1
7
4
8~~CONFIDENTIAL~~



(a) Static tests.

Figure 1.- Conventions used to define positive senses of forces, moments, and angles.

~~CONFIDENTIAL~~

(b) Tunnel tests.

Figure 1.- Concluded.

~~CONFIDENTIAL~~

~~CONFIDENTIAL~~

13

E-1748

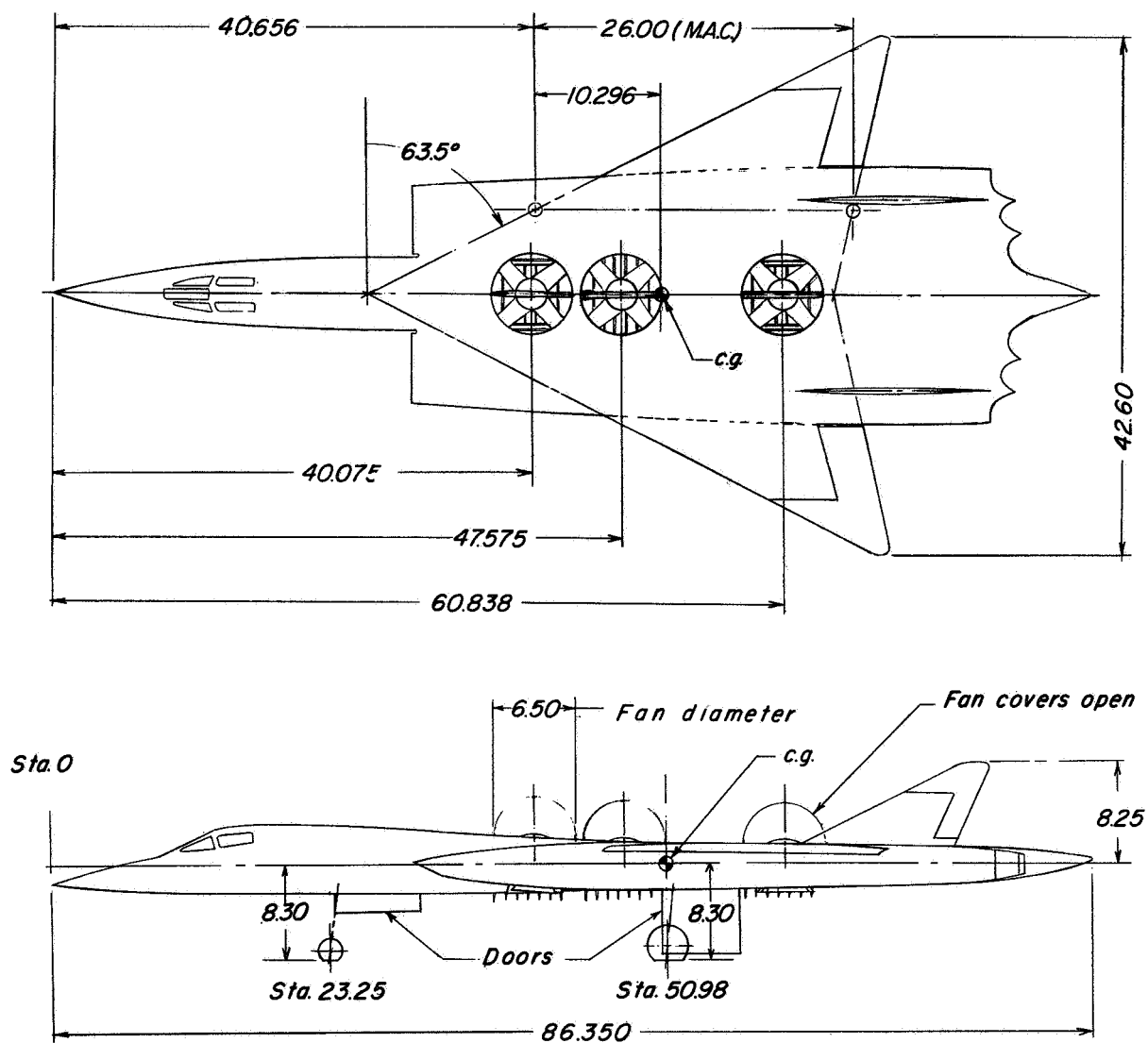
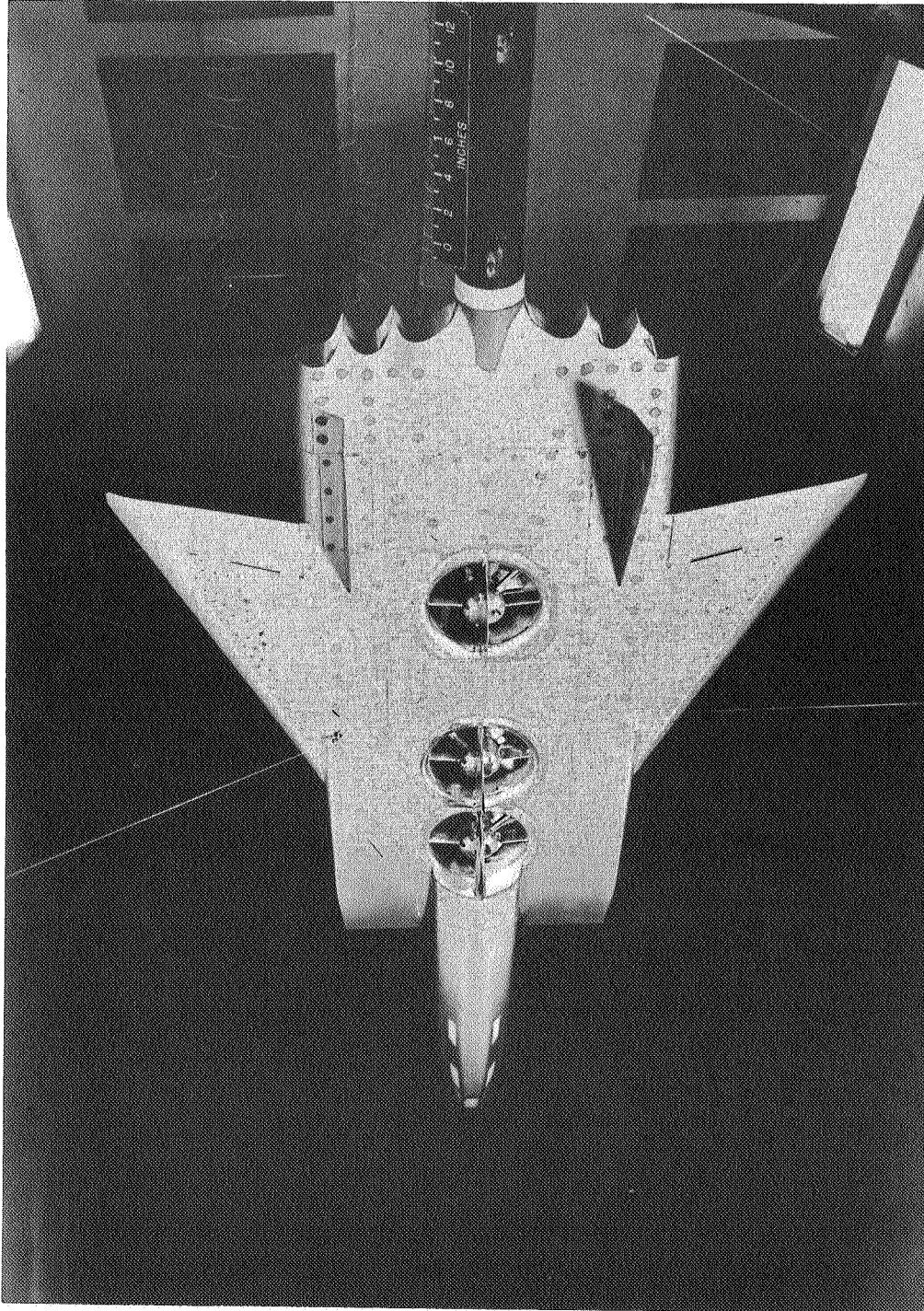


Figure 2.- Sketch of model. All dimensions are in inches.

~~CONFIDENTIAL~~

~~CONFIDENTIAL~~

(a) Top view.

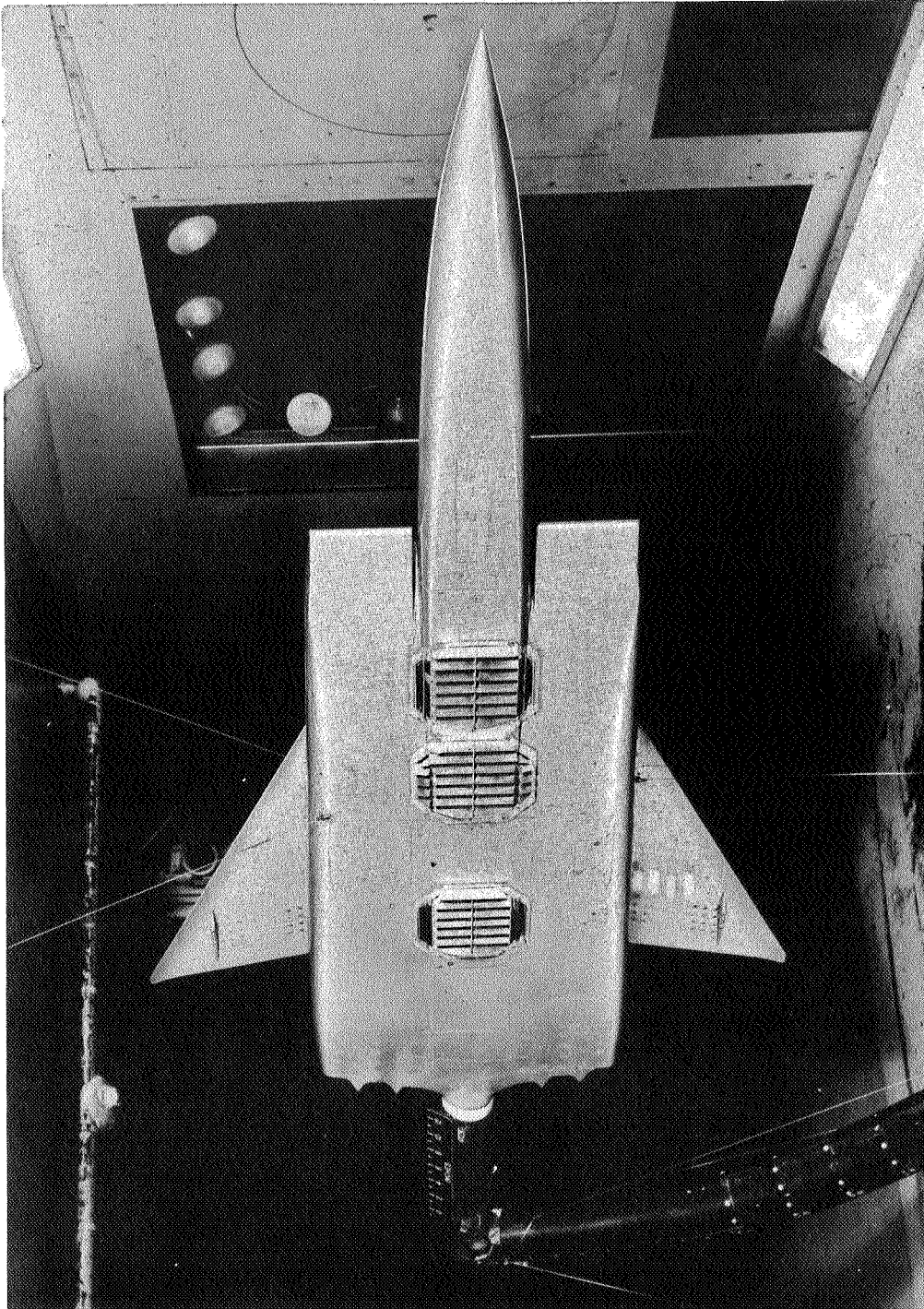
L-60-1326

Figure 3.- Photographs of model in tunnel.

8471-1

~~CONFIDENTIAL~~

L-1748



~~CONFIDENTIAL~~
SECRET

~~CONFIDENTIAL~~
SECRET

L-60-1327

(b) Bottom view.

Figure 3.- Concluded.

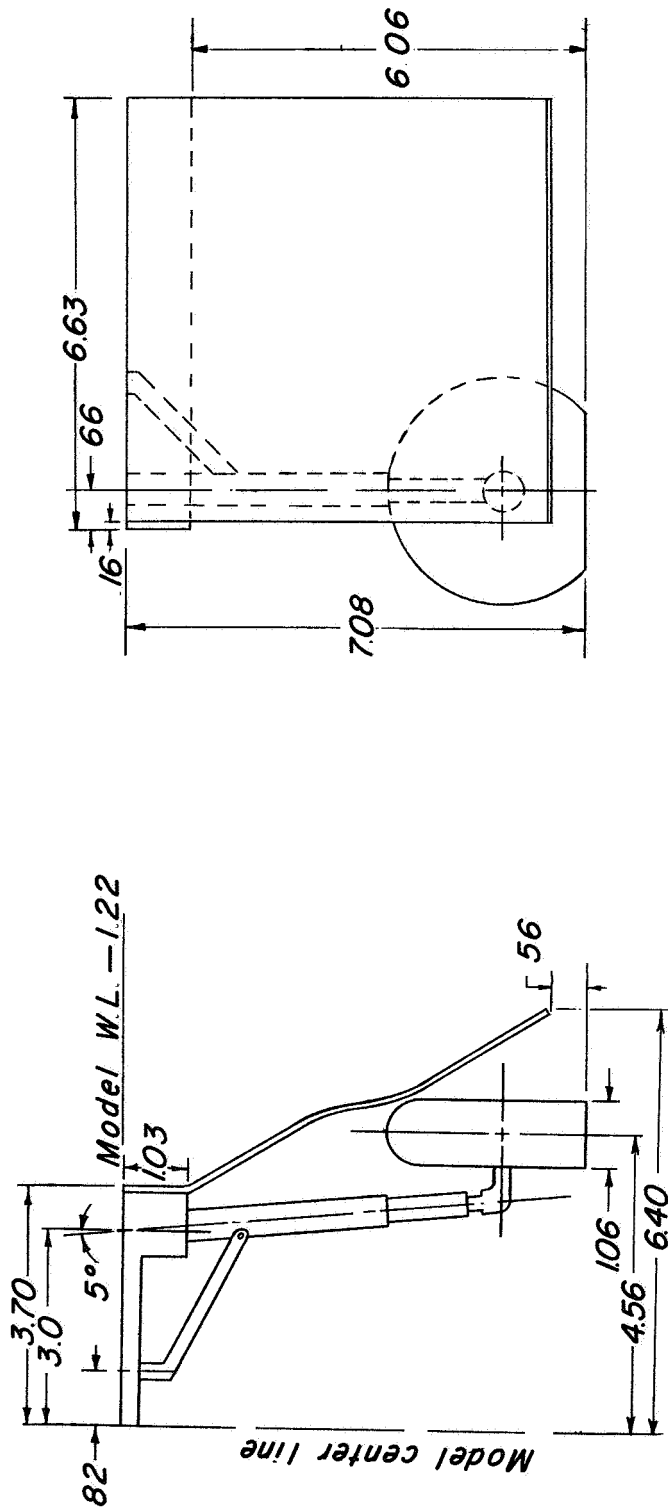
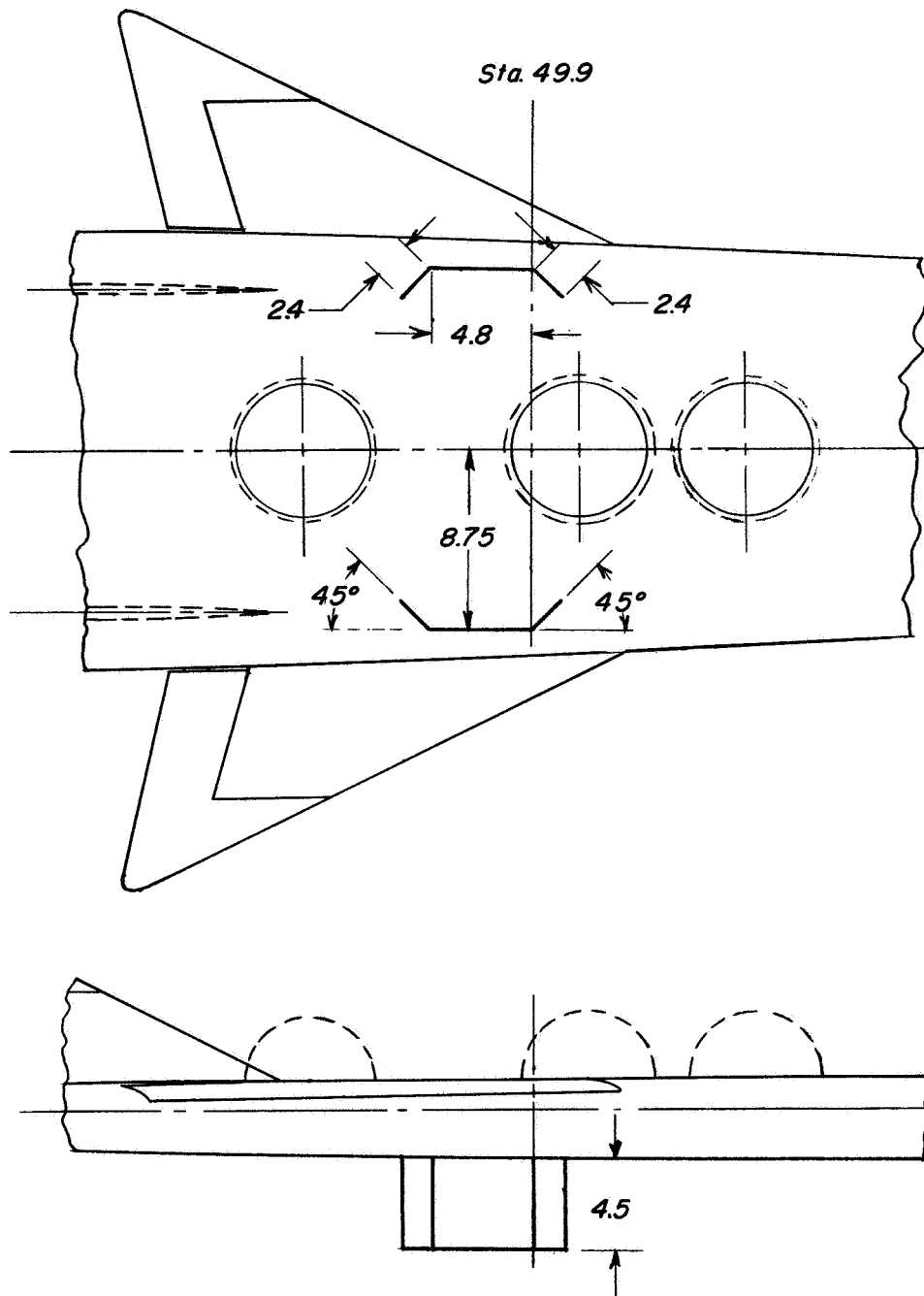


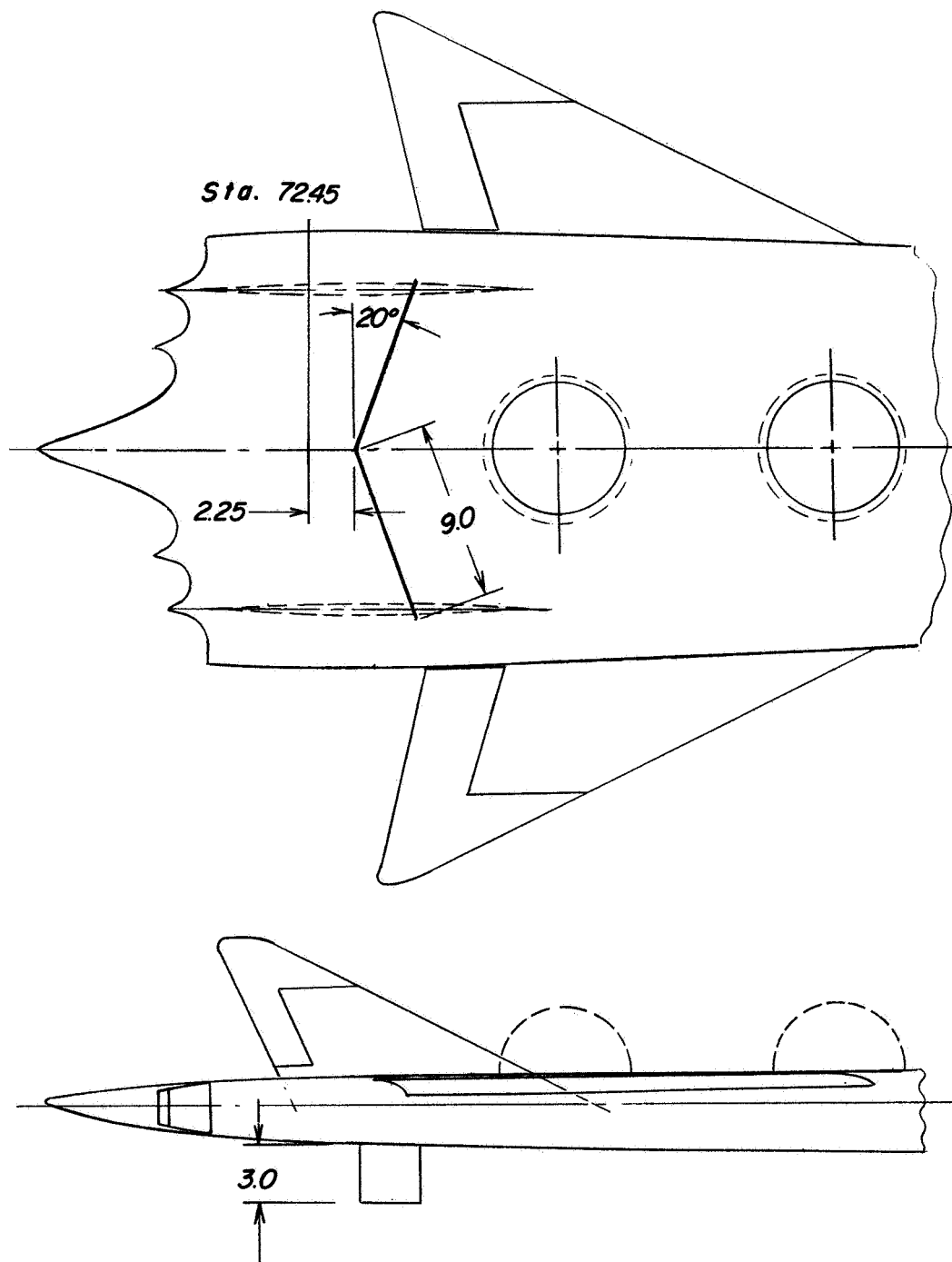
Figure 4.- Details of main landing gear and doors employed on model.
All dimensions are in inches.

~~CONFIDENTIAL~~

(a) Fence 1.

Figure 5.- Sketches of fences used on model. All dimensions are in inches.

~~CONFIDENTIAL~~

~~CONFIDENTIAL~~

(b) Fence 2.

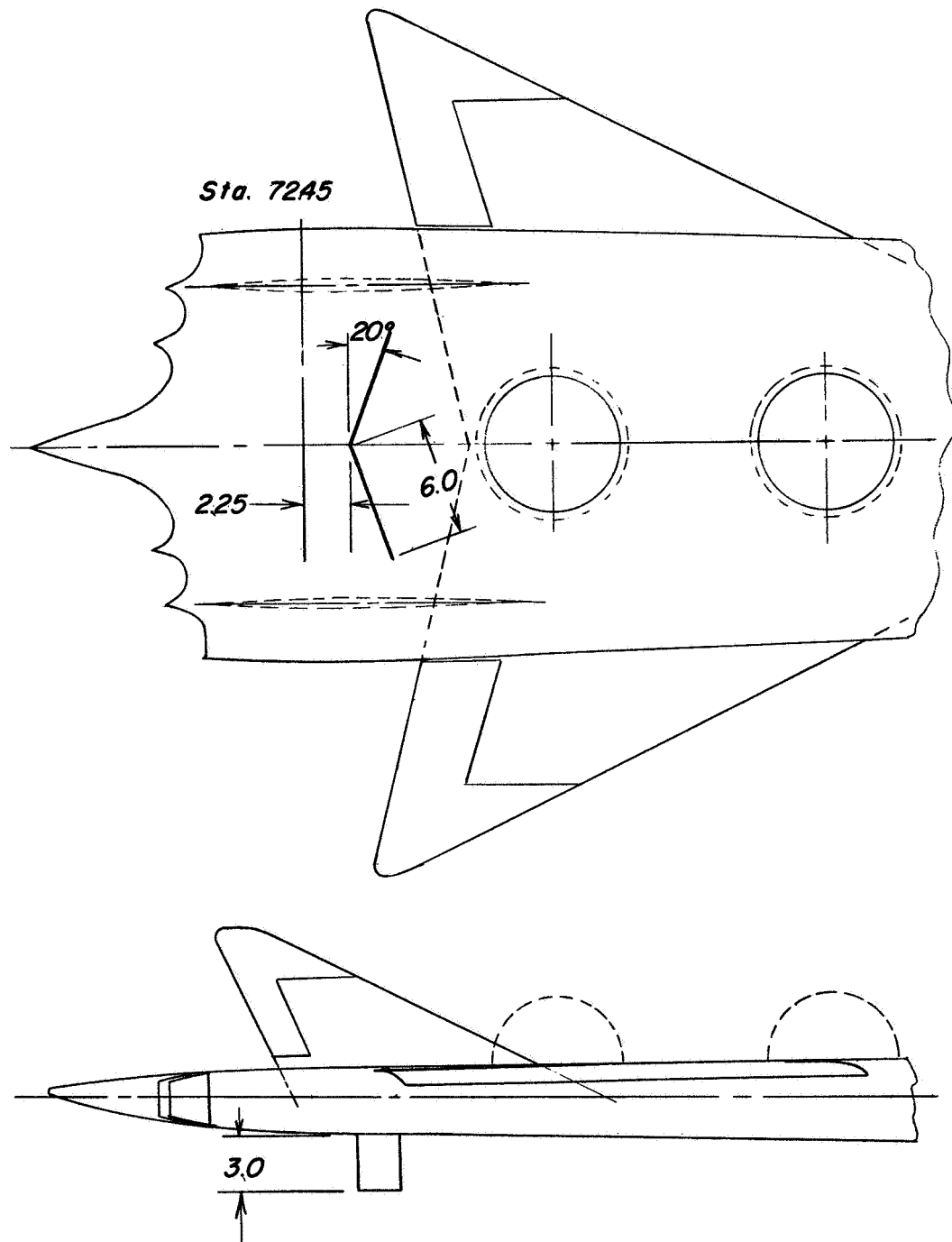
Figure 5.- Continued.

~~CONFIDENTIAL~~

I-1748

~~CONFIDENTIAL~~

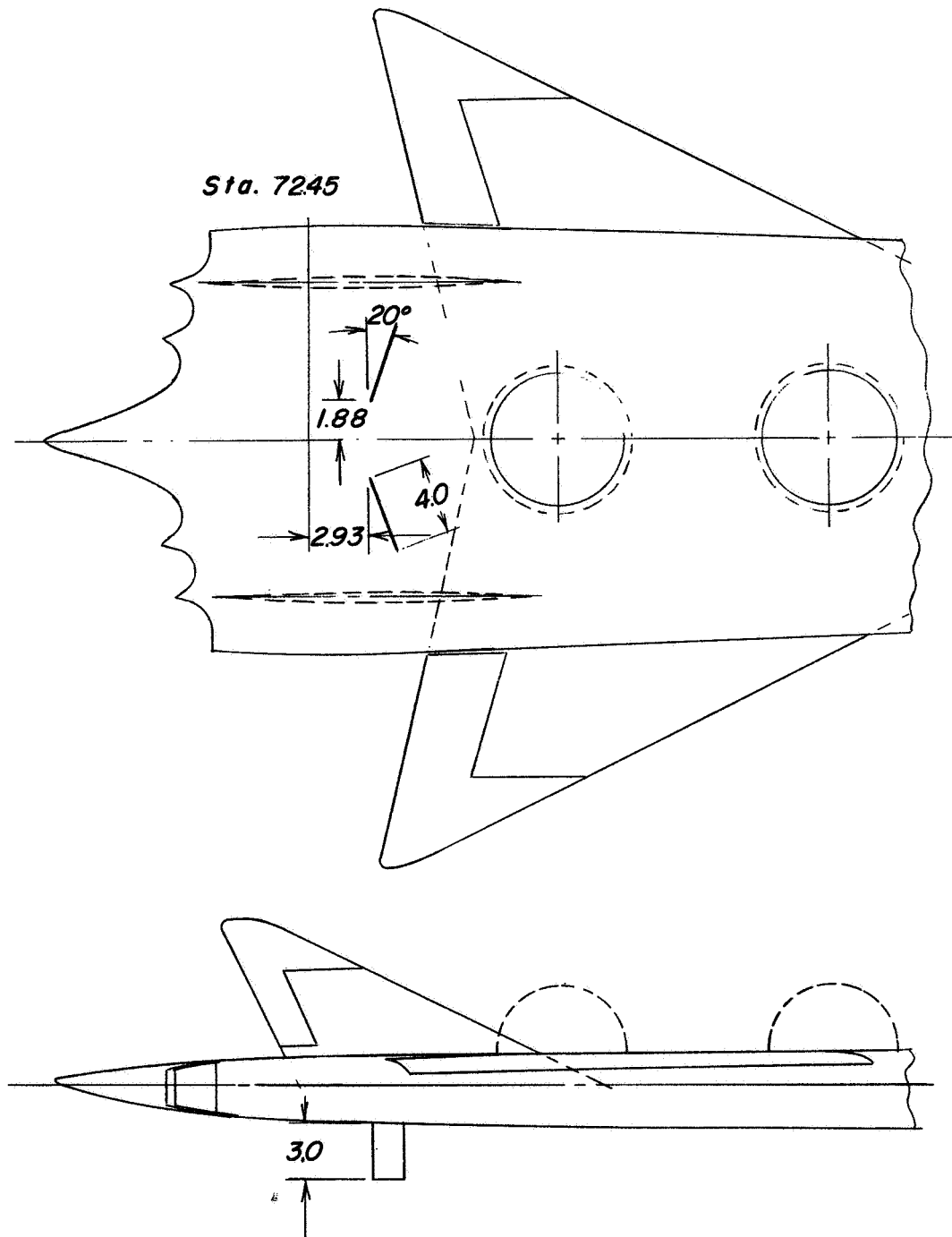
L-1748



(c) Fence 3.

Figure 5.- Continued.

~~CONFIDENTIAL~~

~~CONFIDENTIAL~~

L-1748

(d) Fence 4.

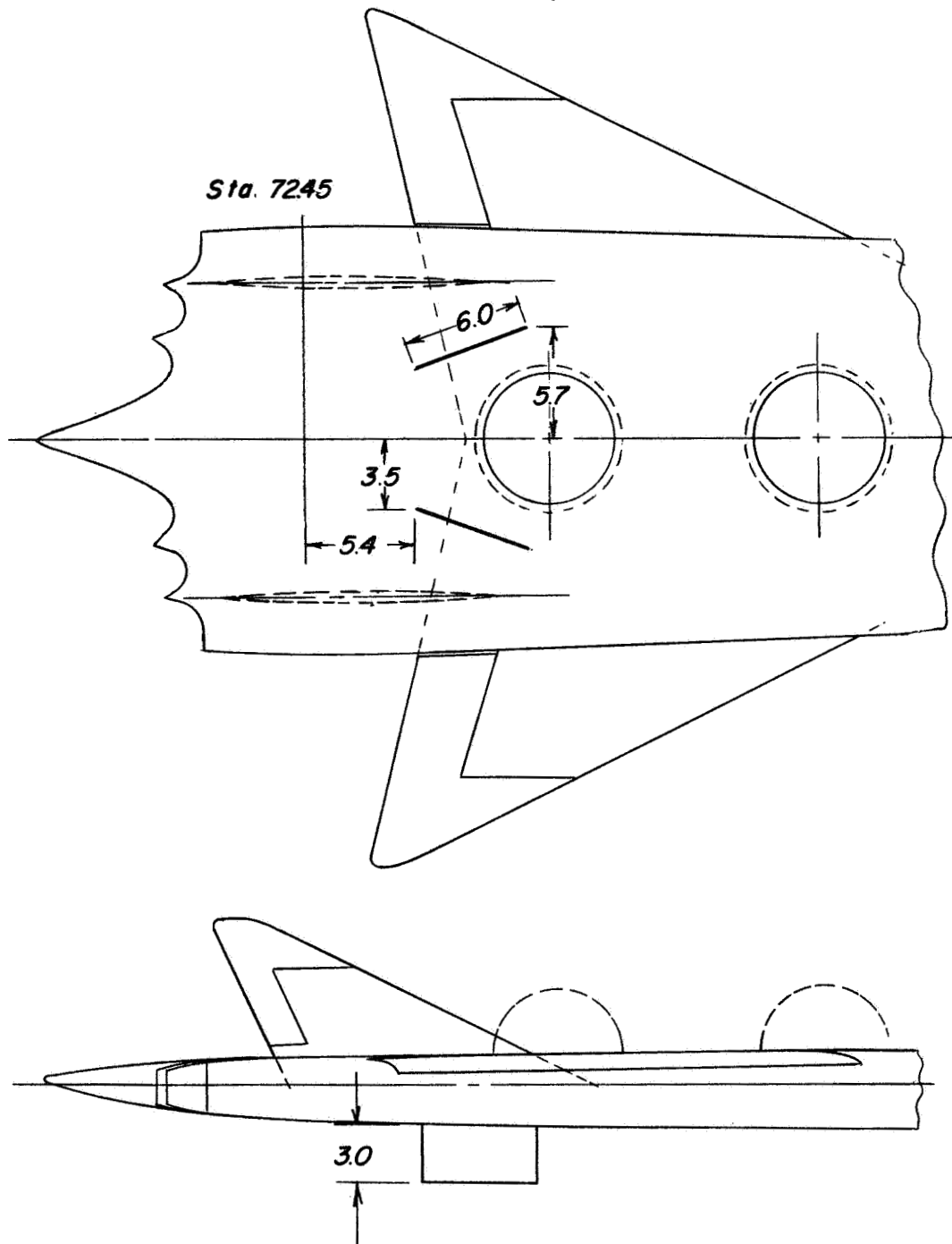
Figure 5.- Continued.

~~CONFIDENTIAL~~

~~CONFIDENTIAL~~

21

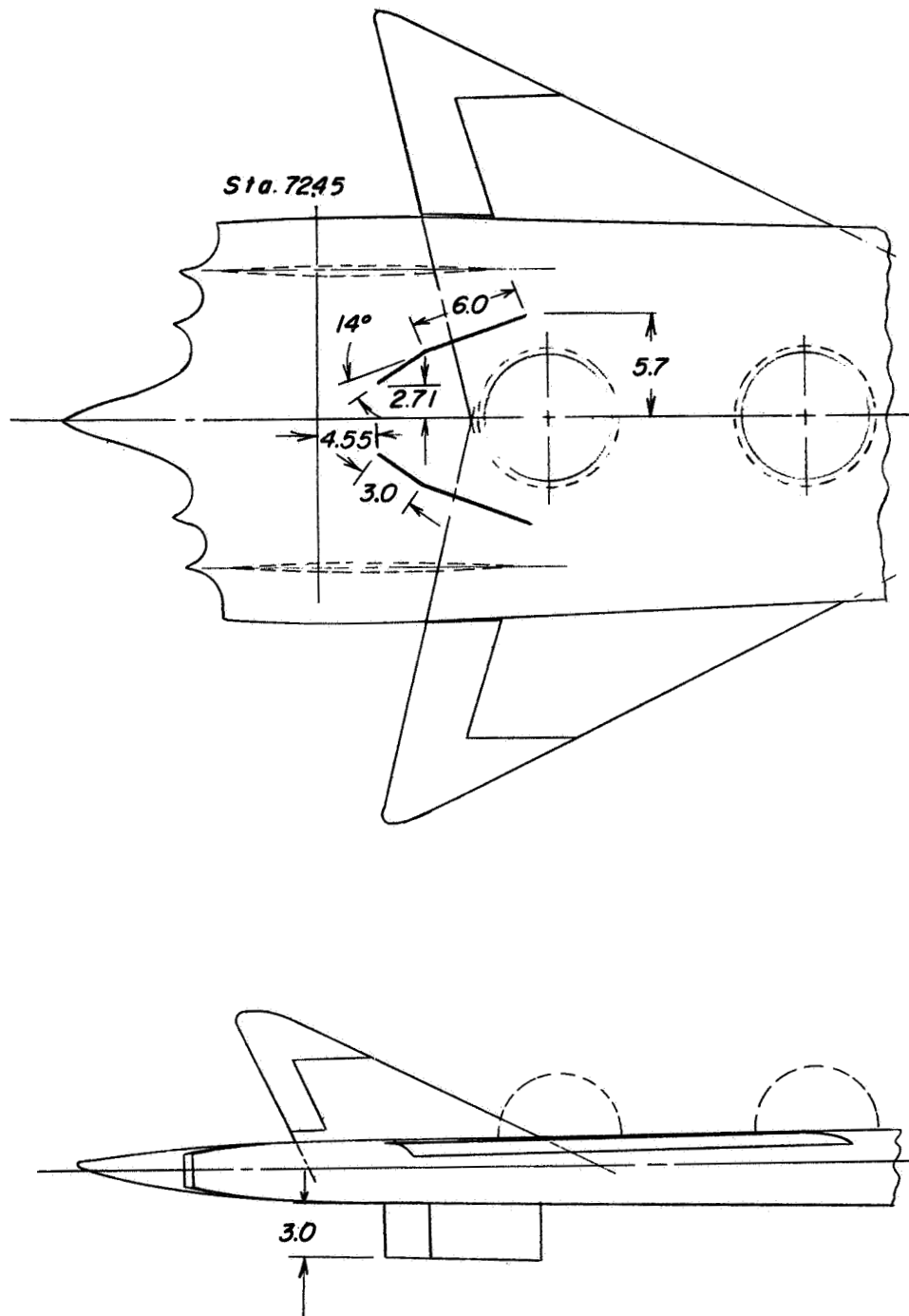
L-1748



(e) Fence 5.

Figure 5.- Continued.

~~CONFIDENTIAL~~

~~CONFIDENTIAL~~

(f) Fence 6.

Figure 5.- Concluded.

~~CONFIDENTIAL~~

~~CONFIDENTIAL~~

I-1748

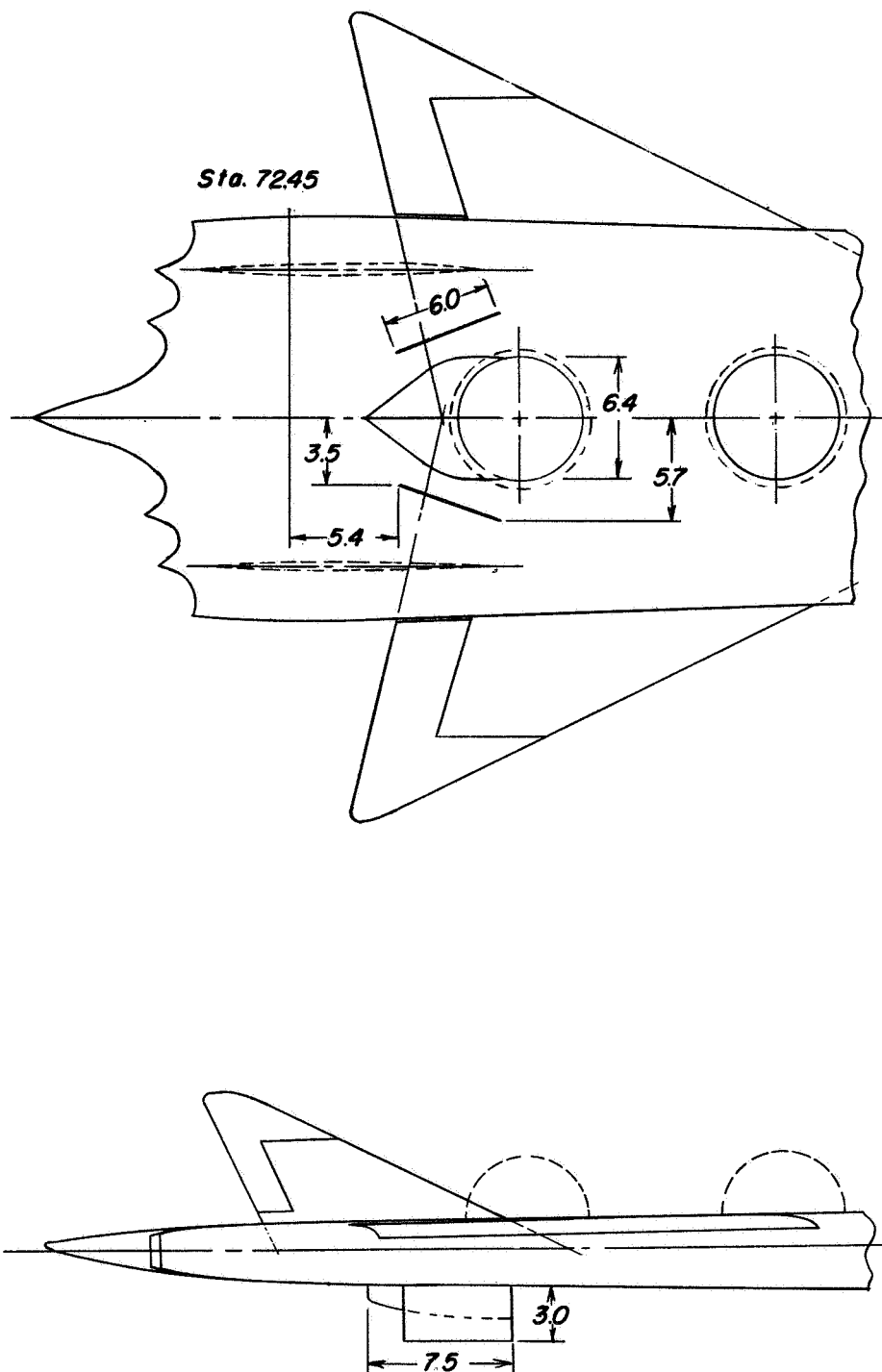
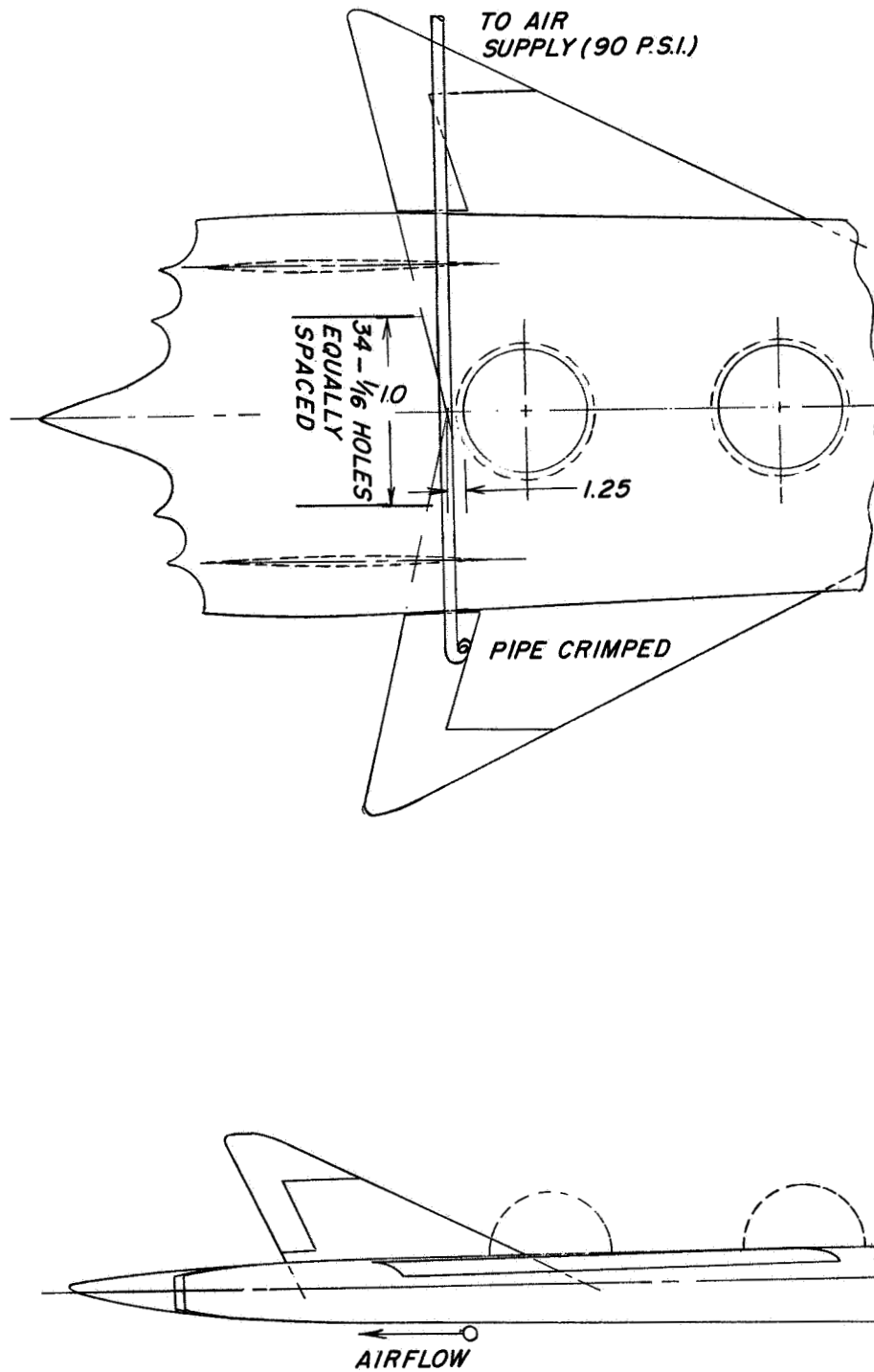


Figure 6.- Details of boattail body employed with fence 5.
All dimensions are in inches.

~~CONFIDENTIAL~~

~~CONFIDENTIAL~~

L-1748

Figure 7.- Details of boundary-layer control device behind rear fan.
All dimensions are in inches.

~~CONFIDENTIAL~~

~~CONFIDENTIAL~~

I-1748

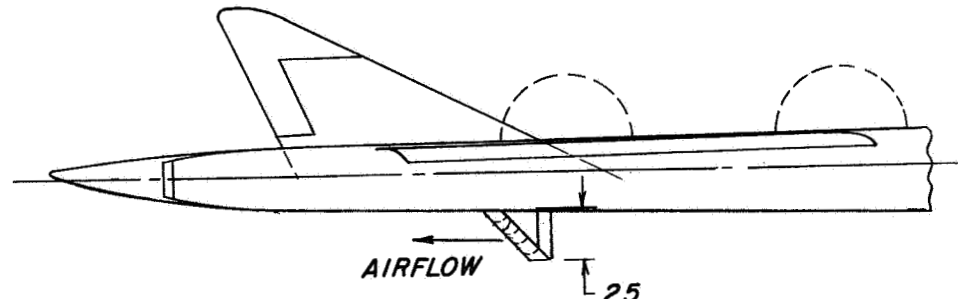
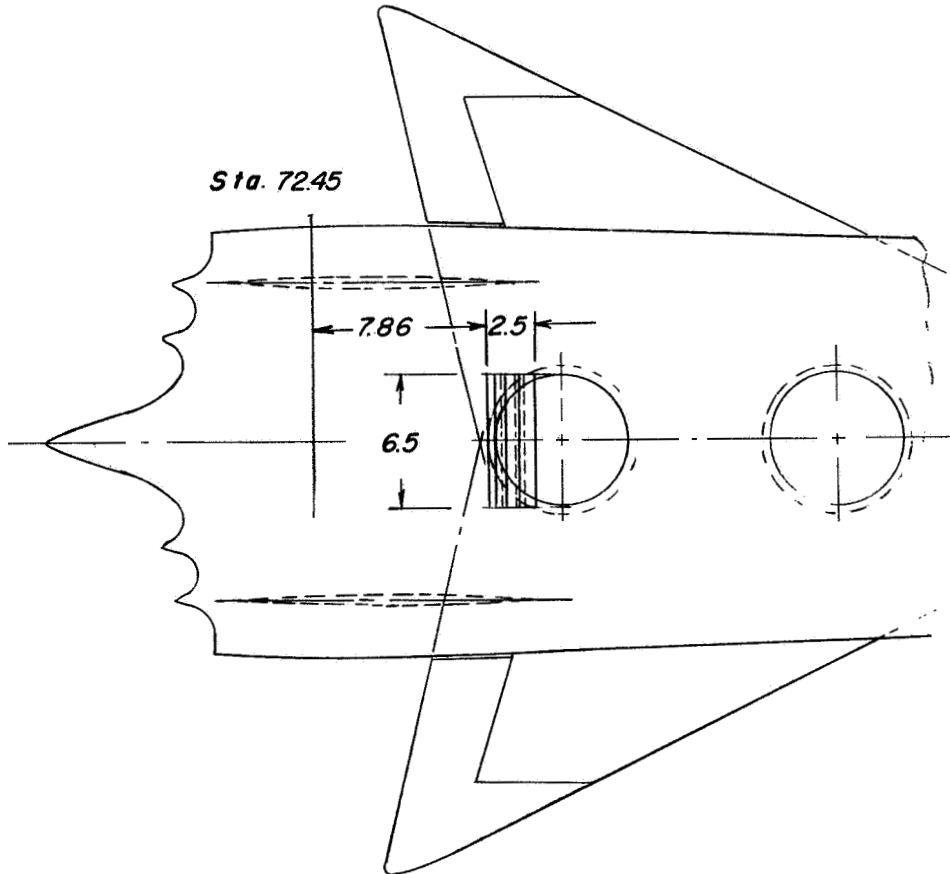


Figure 8.- Details of 45° cascade used on rear fan. All dimensions are in inches.

~~CONFIDENTIAL~~

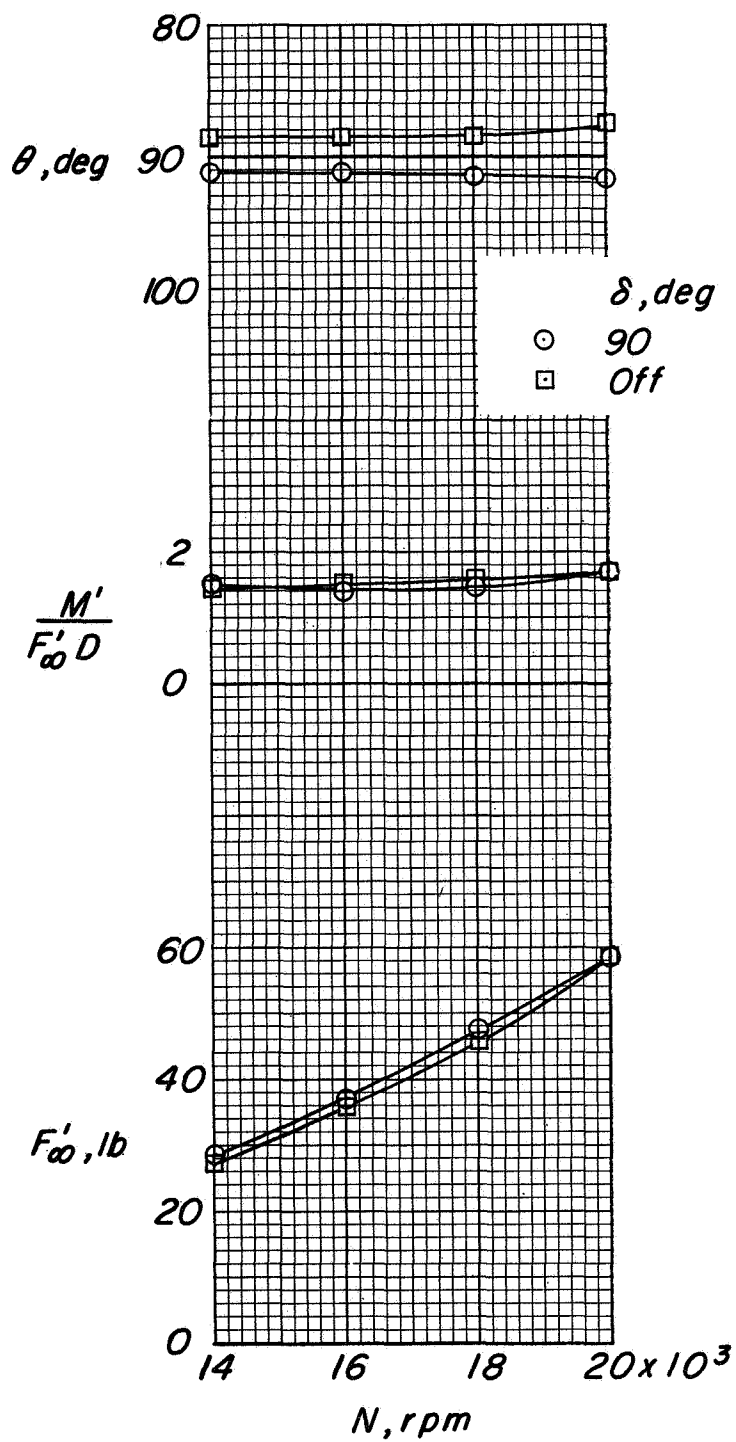
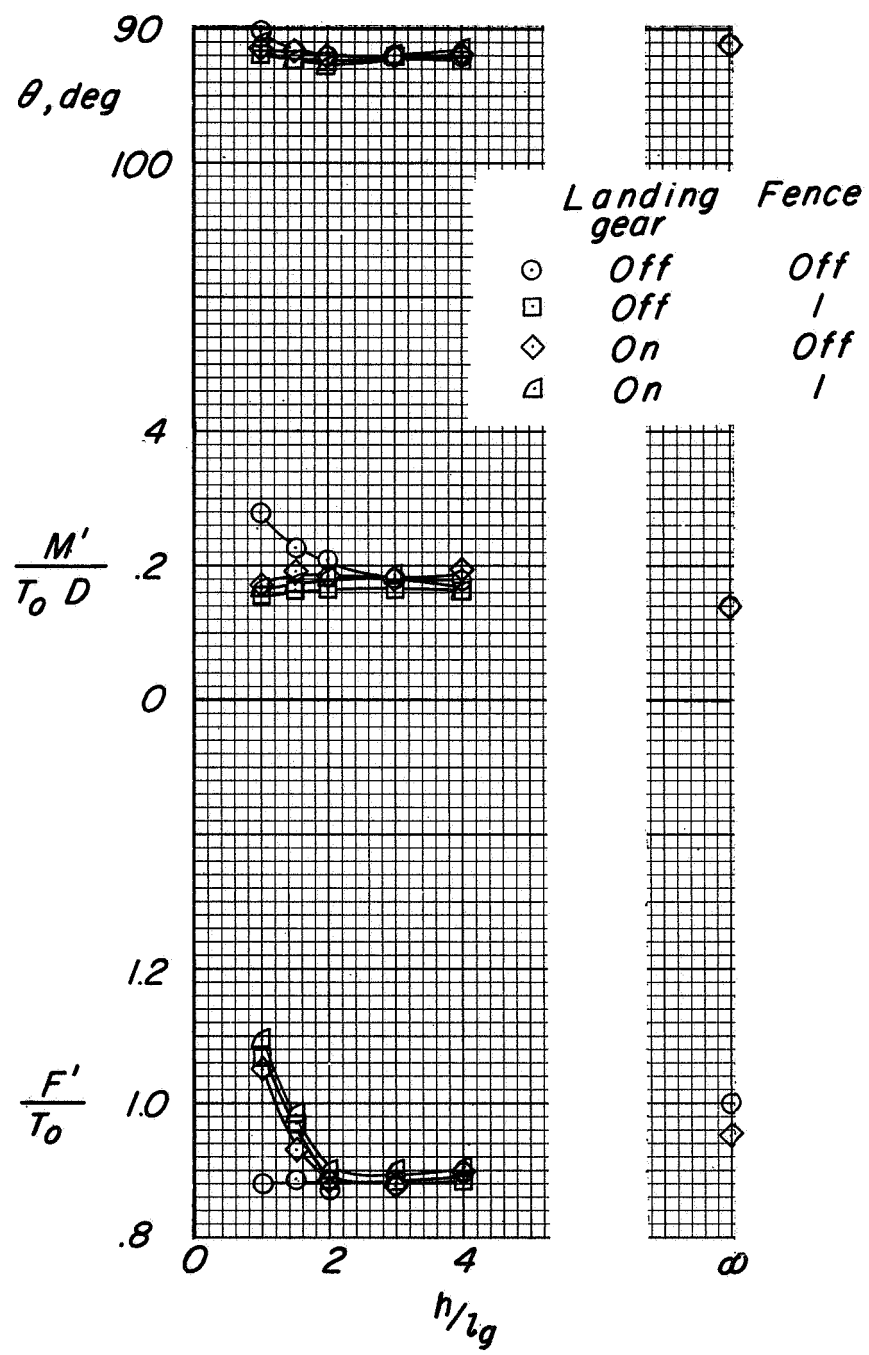


Figure 9.- Calibration of fans. $V_\infty/V_j = 0$; $\gamma = 0^\circ$; $h/l_g = \infty$.

CONFIDENTIAL

~~CONFIDENTIAL~~

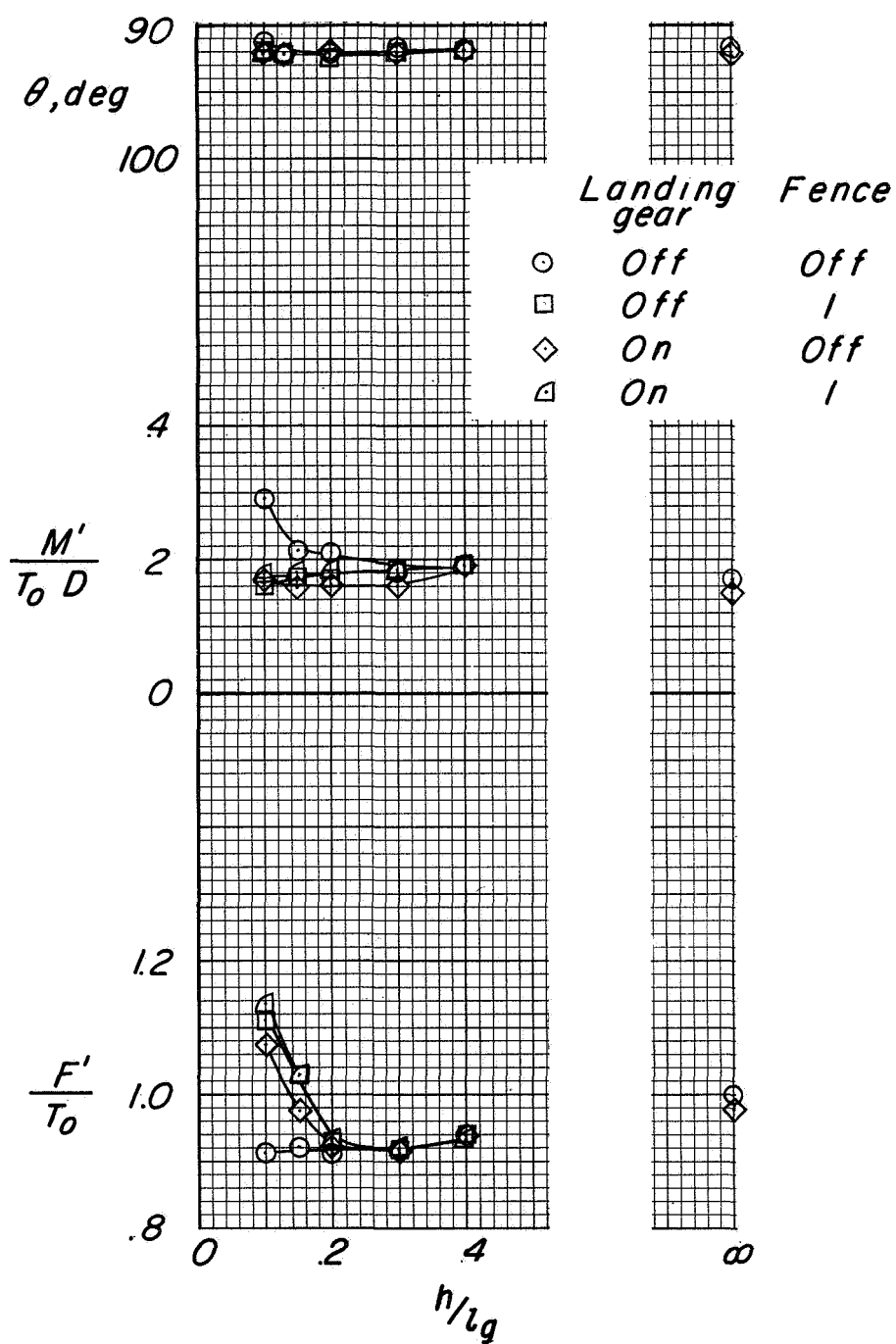
L-1748



(a) $N = 16,000$ rpm.

Figure 10.- Effect of height above ground for various model conditions.
 $\delta = 90^\circ$; $\gamma = 0^\circ$.

~~CONFIDENTIAL~~



(b) $N = 20,000$ rpm.

Figure 10.- Concluded.

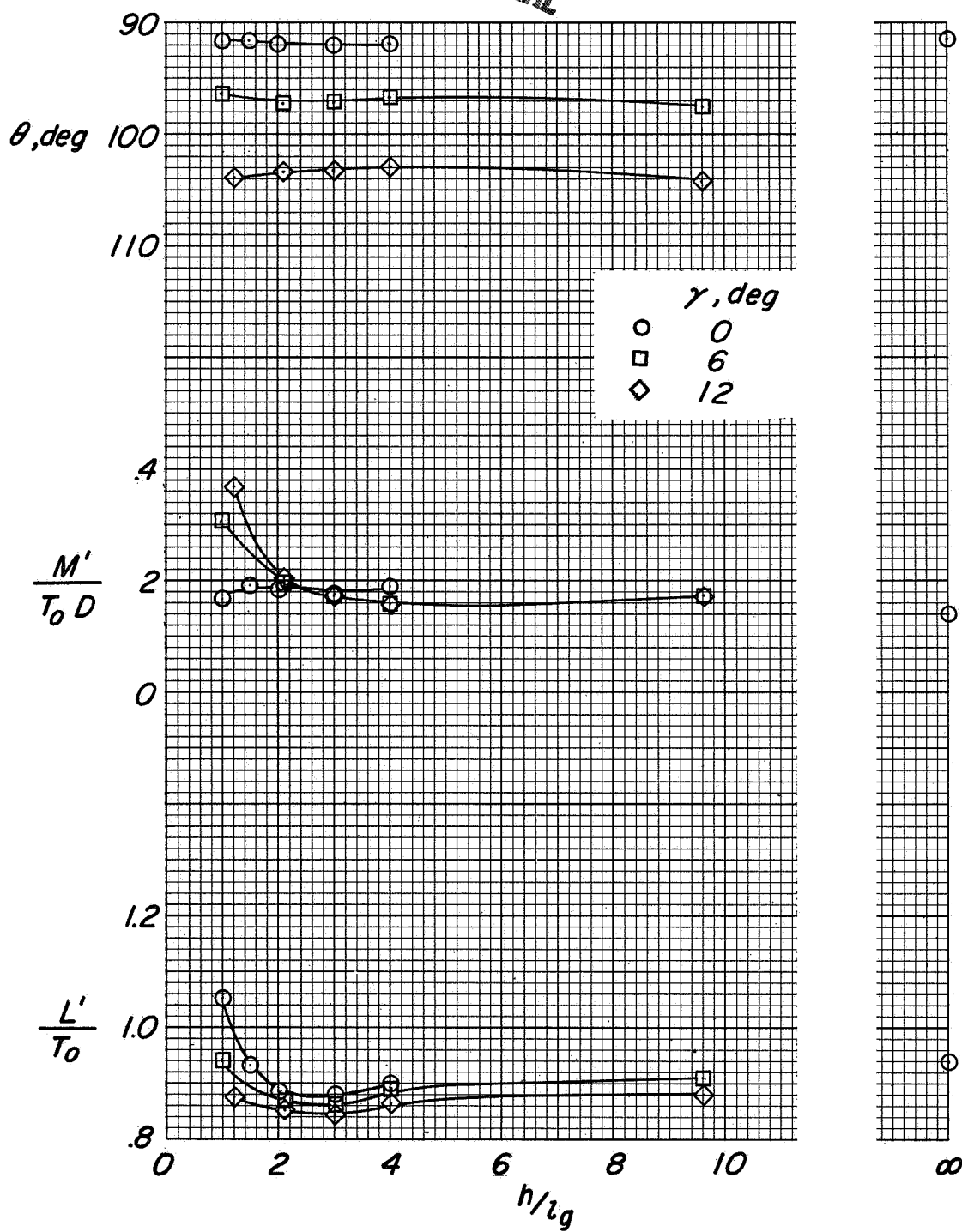


Figure 11.- Effect of height above ground at various model attitudes.
Landing gear on; $\delta = 90^\circ$; $V_\infty/V_j = 0$; $N = 16,000$ rpm.

~~CONFIDENTIAL~~

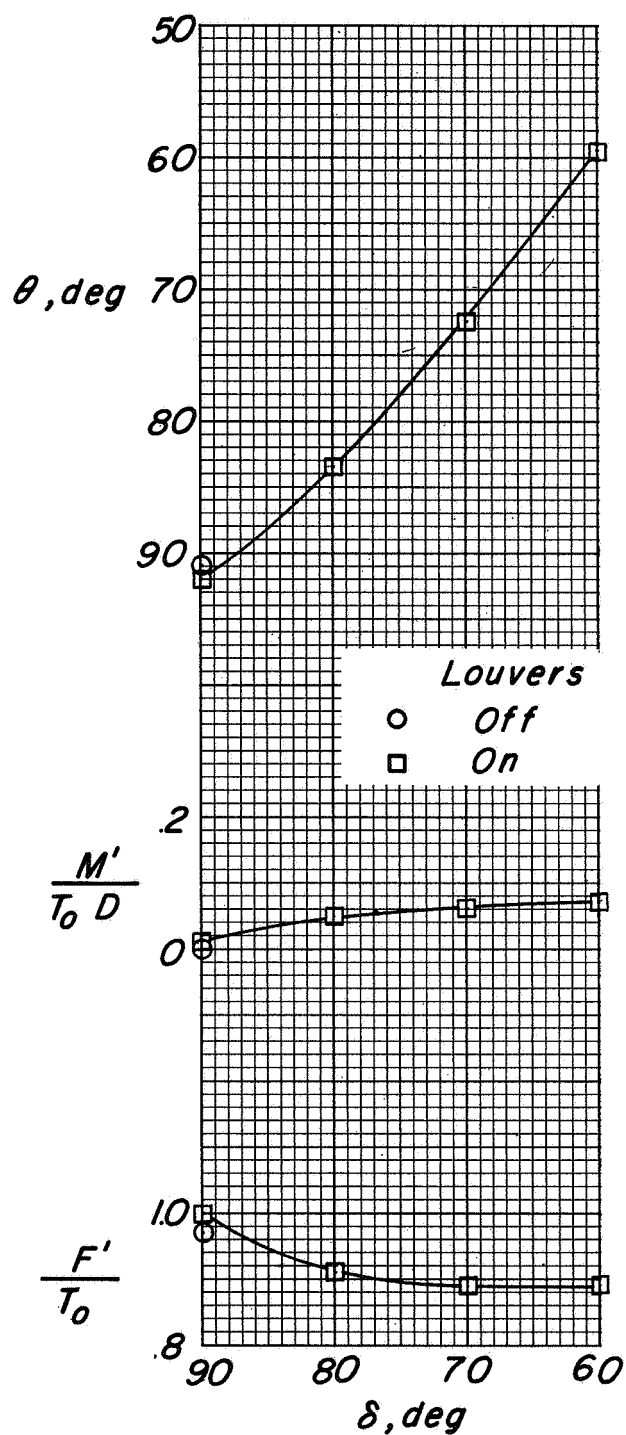


Figure 12.- Effect of louver angle on fan characteristics. Midfan;
 $\gamma = 0^\circ$; $N = 18,000$ rpm; moment reference at center line of fan.

~~CONFIDENTIAL~~

L-1748

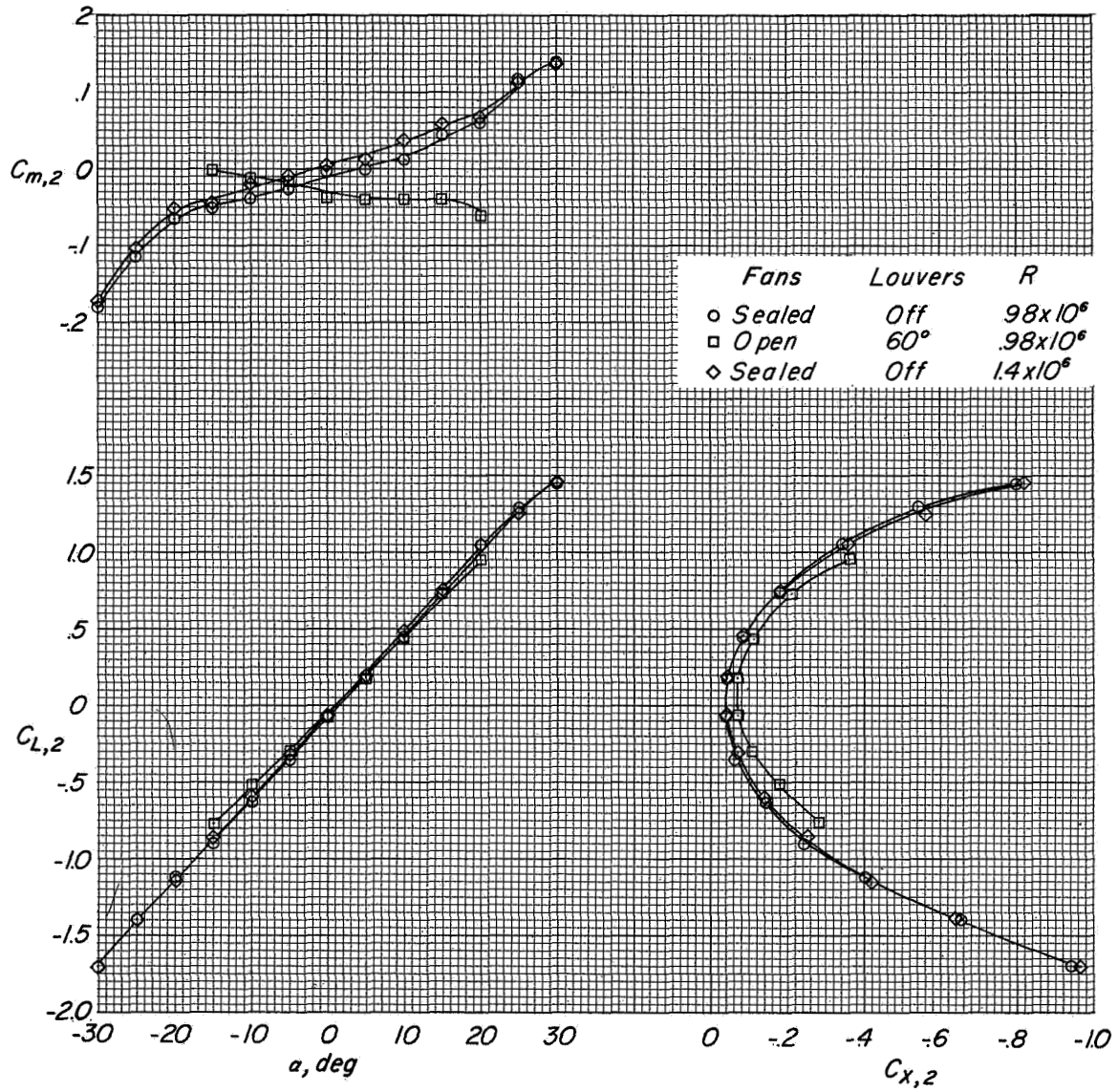


Figure 13.- Basic aerodynamic characteristics of model with fan inlets and exits opened and sealed. $V_\infty/V_j = \infty$.

~~CONFIDENTIAL~~

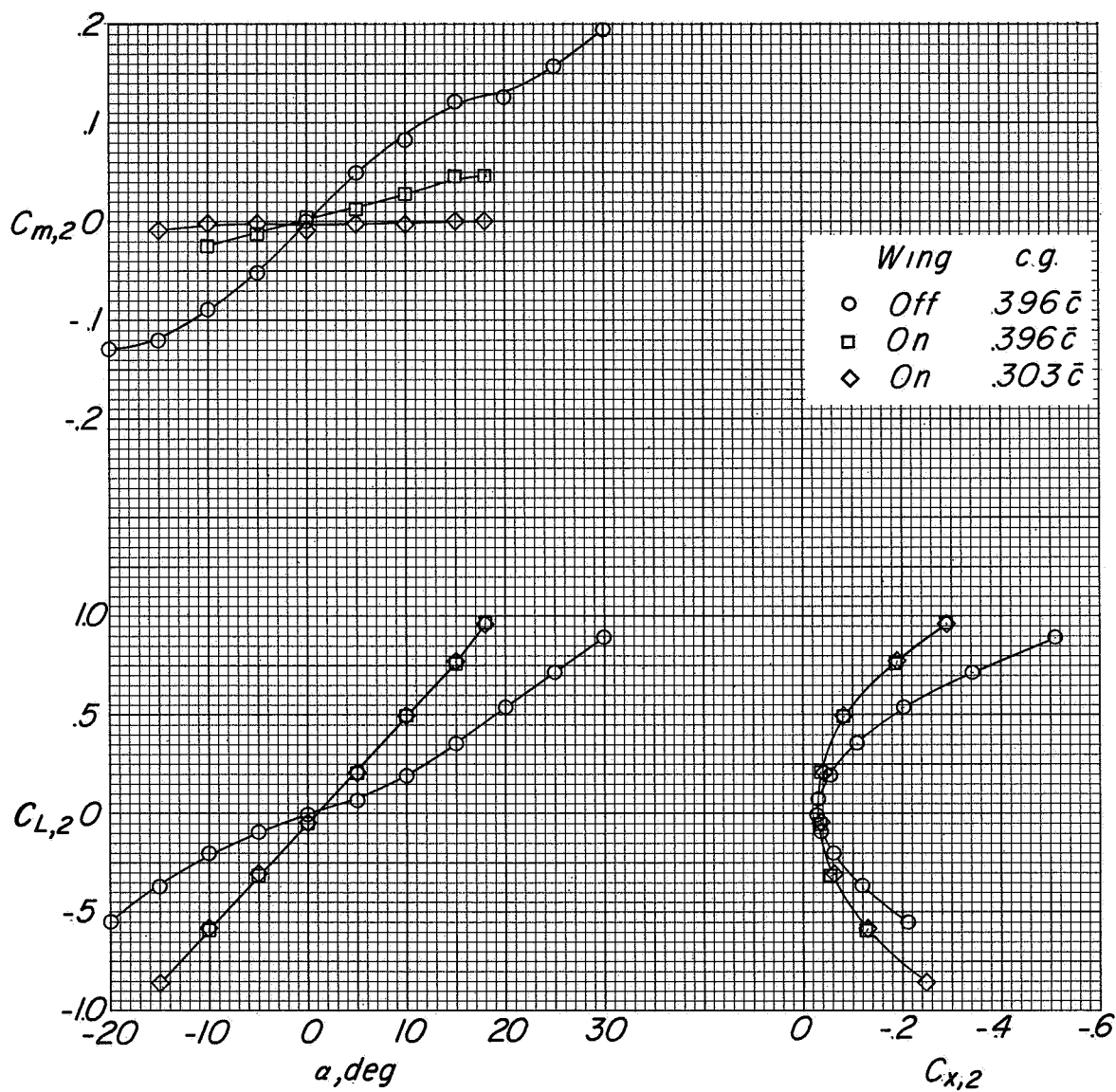
~~CONFIDENTIAL~~

Figure 14.- Effect of wing off and chordwise movement of wing on aerodynamic characteristics. $V_\infty/V_j = \infty$; fan inlets and exits sealed.

~~CONFIDENTIAL~~

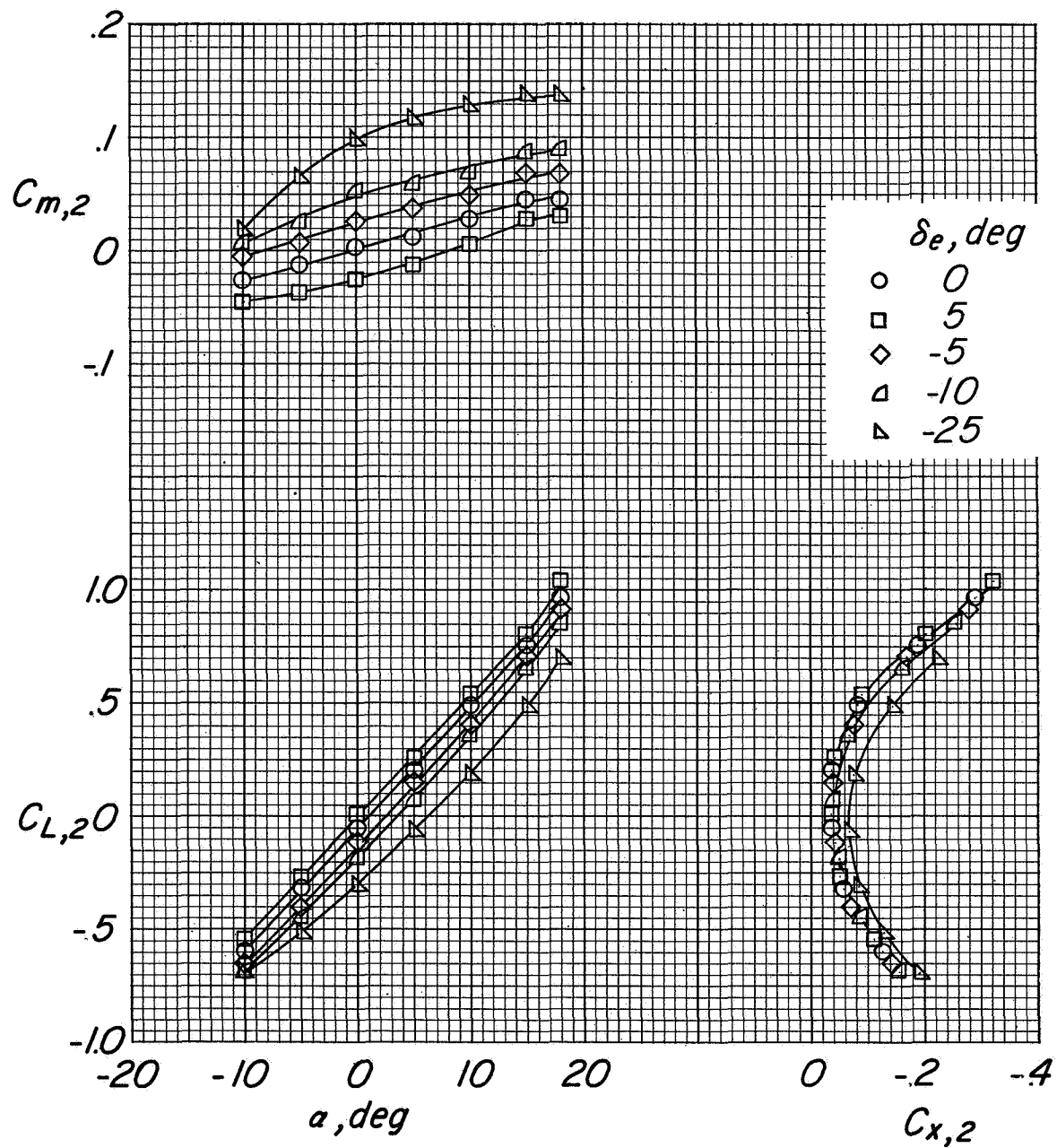
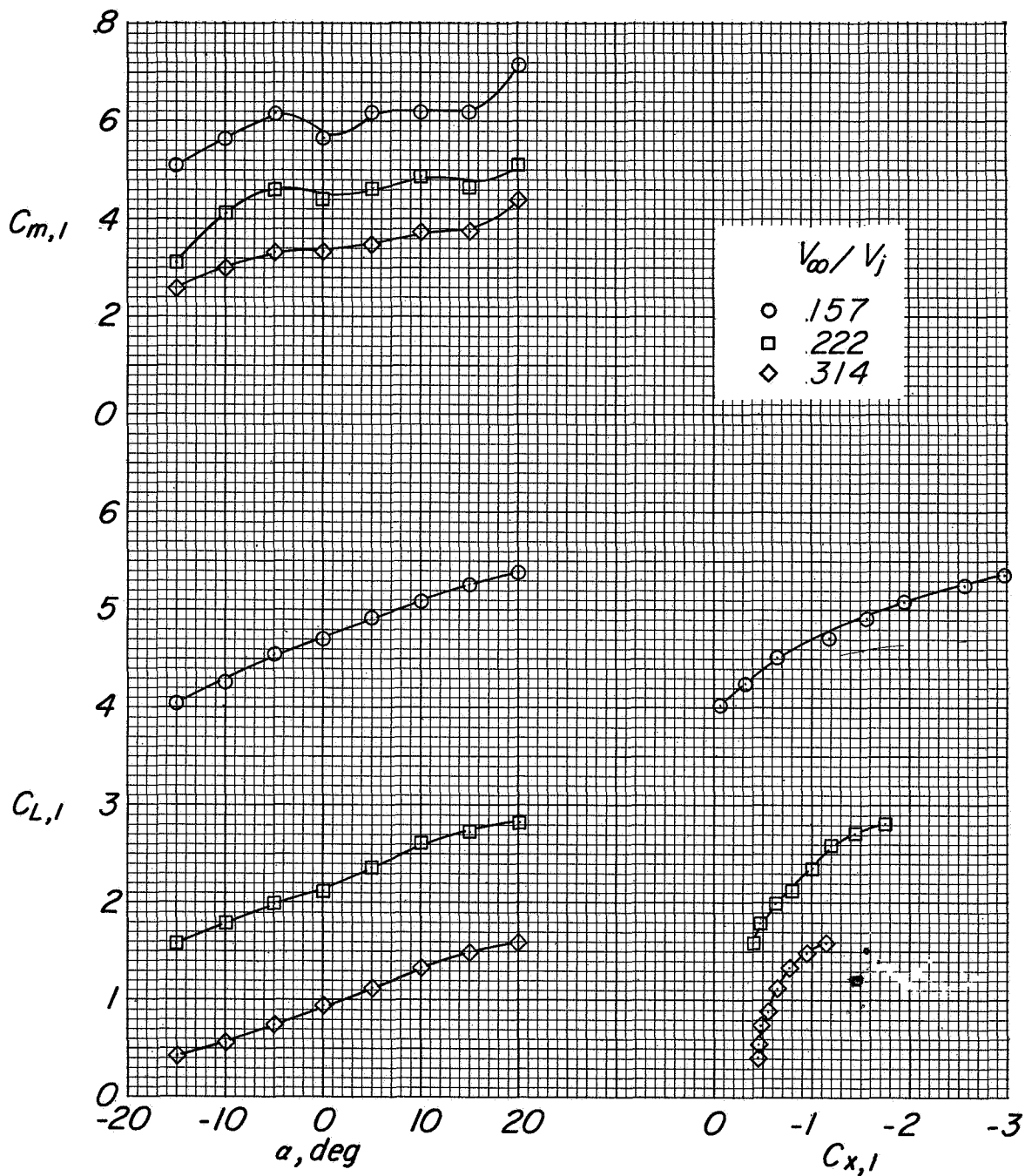
~~CONFIDENTIAL~~

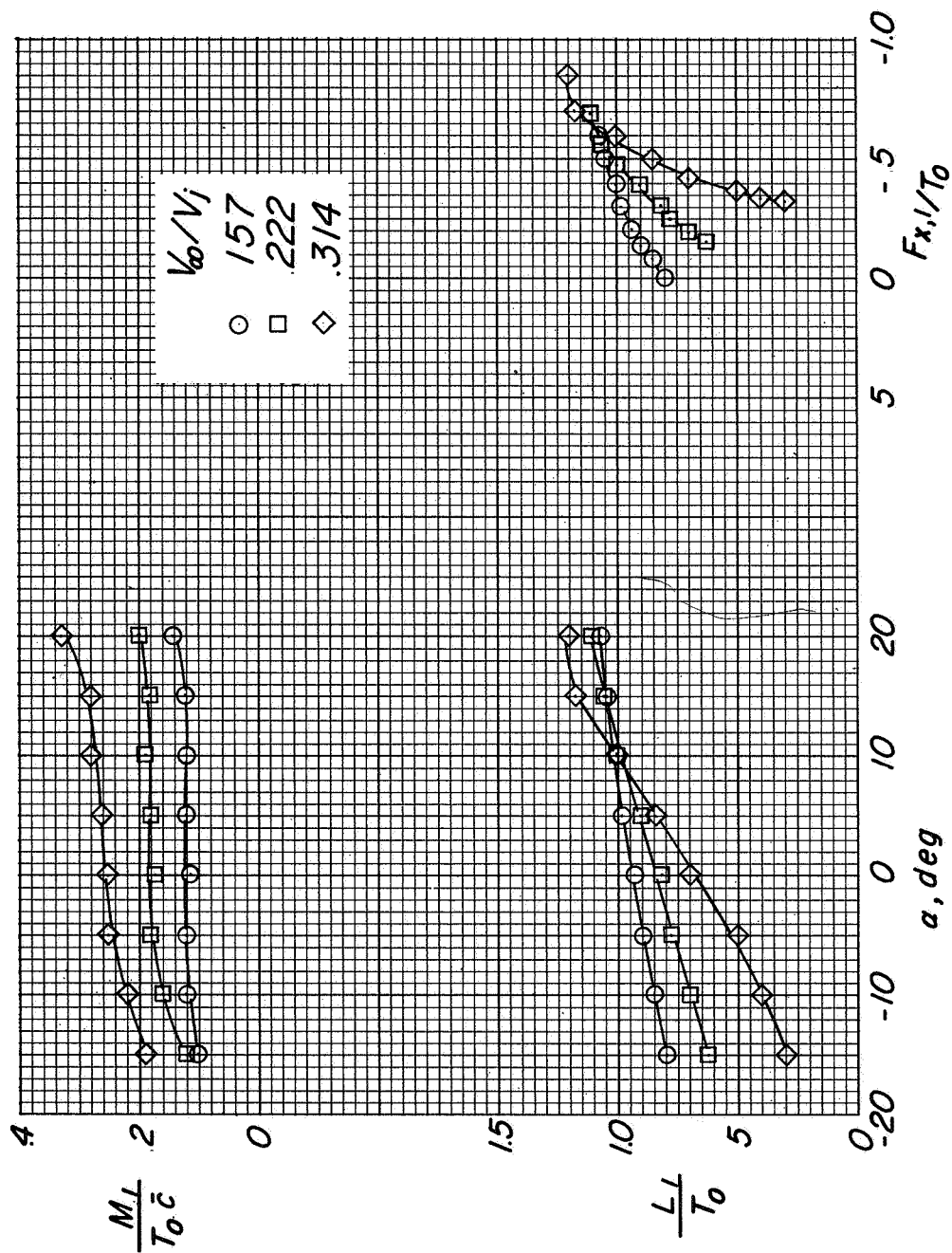
Figure 15.- Elevator effectiveness. $V_\infty/V_j = \infty$; louvers off.

~~CONFIDENTIAL~~



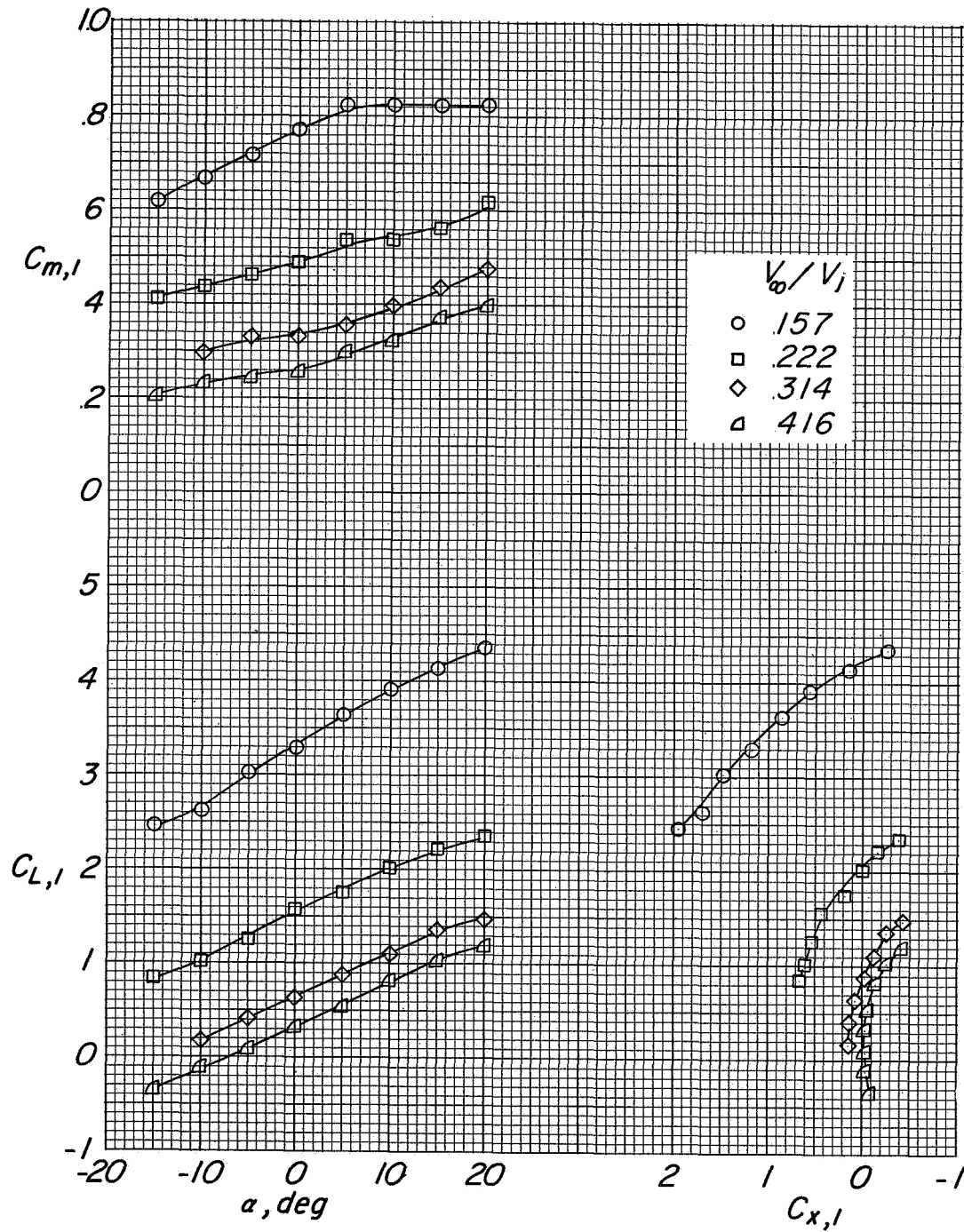
(a) Longitudinal coefficients.

Figure 16.- Basic aerodynamic characteristics. $\delta = 90^\circ$.



(b) Longitudinal forces and moments.

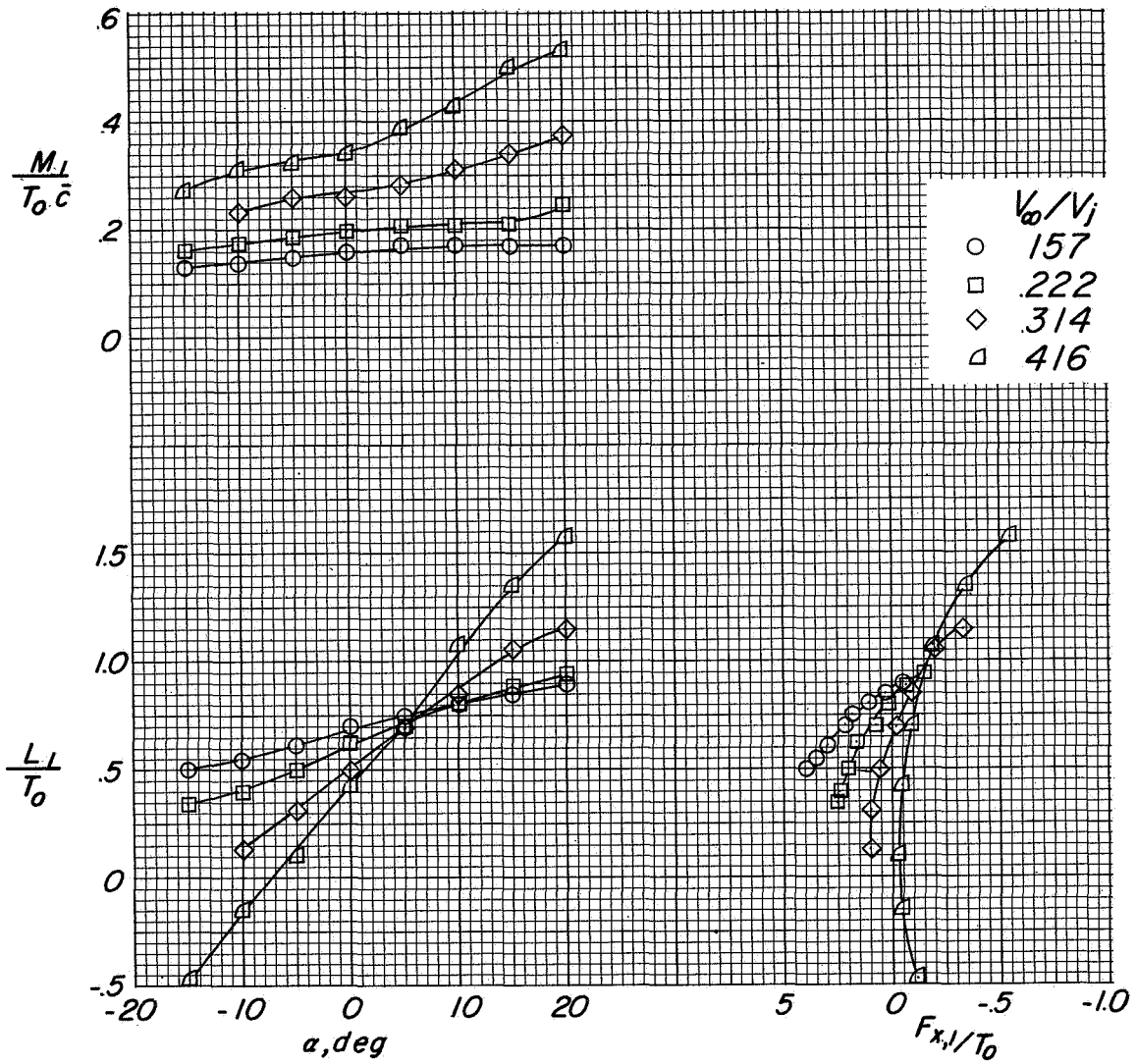
Figure 16.- Concluded.

~~CONFIDENTIAL~~

(a) Longitudinal coefficients.

Figure 17.- Basic aerodynamic characteristics. $\delta = 60^\circ$.~~CONFIDENTIAL~~

~~CONFIDENTIAL~~

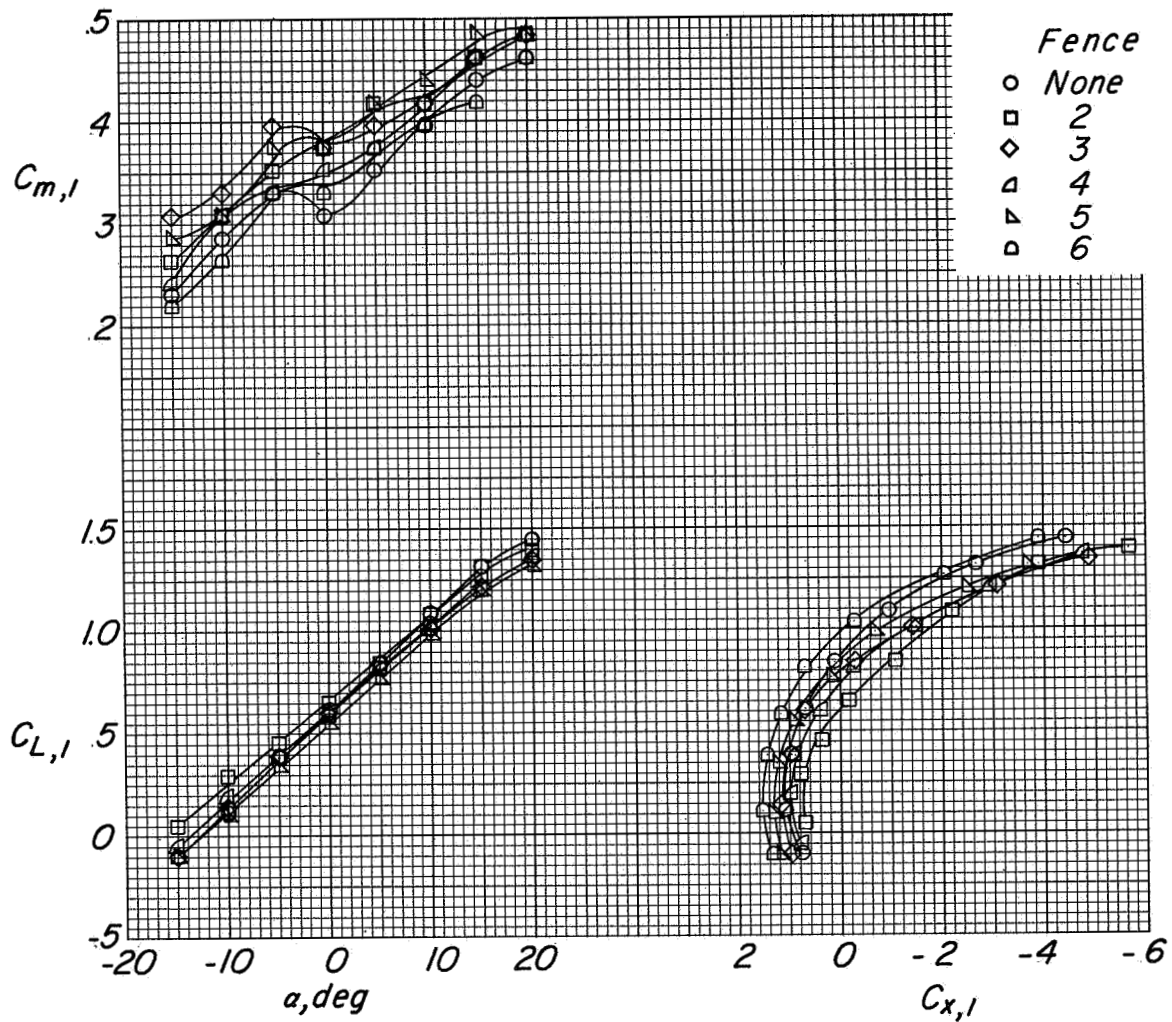


(b) Longitudinal forces and moments.

Figure 17.- Concluded.

~~CONFIDENTIAL~~

CONFIDENTIAL



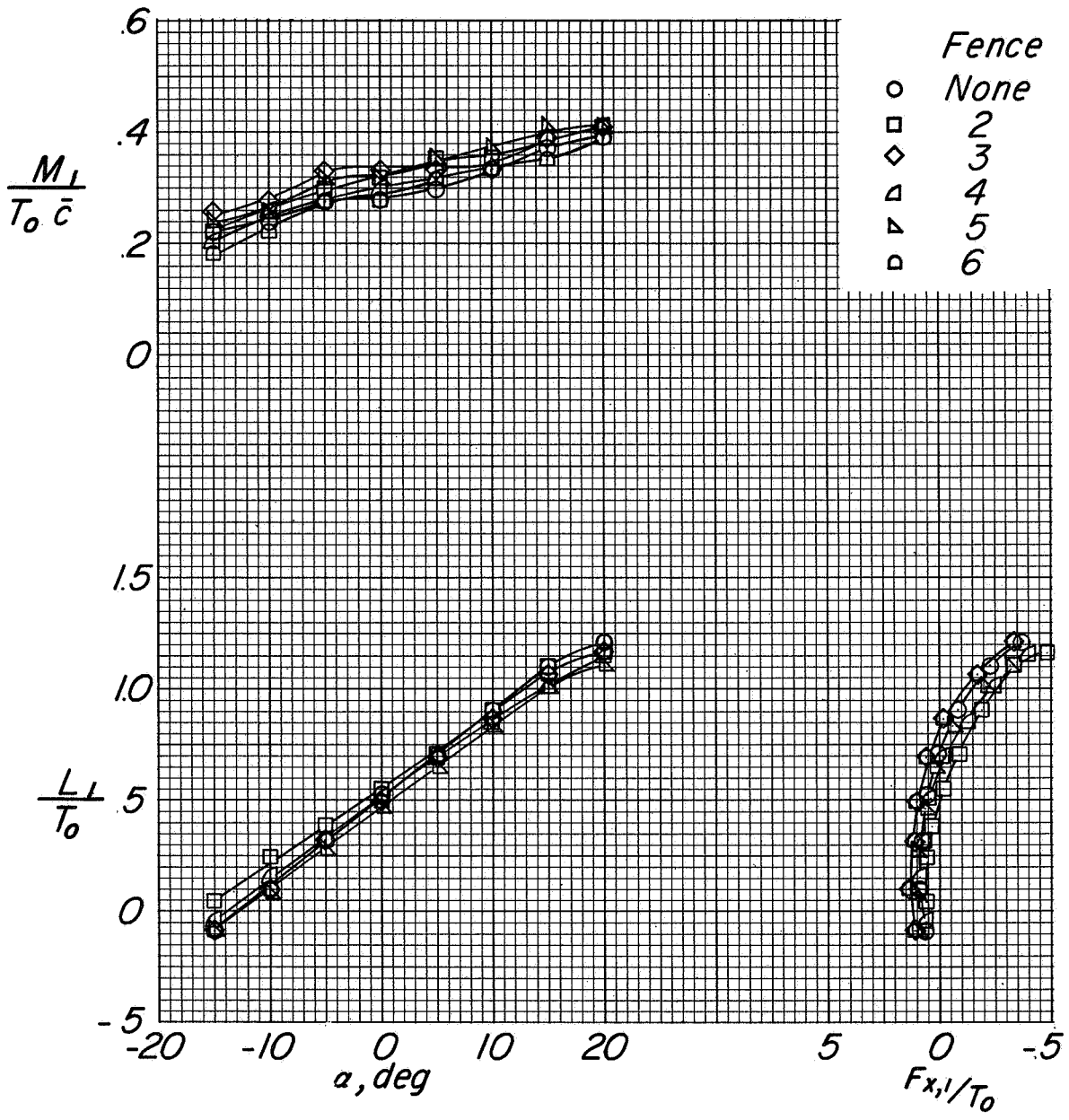
(a) Longitudinal coefficients.

Figure 18.- Effect of various lower-surface fences on aerodynamic characteristics. $V_\infty/V_j = 0.316$; $\delta = 60^\circ$.

CONFIDENTIAL

I-1748

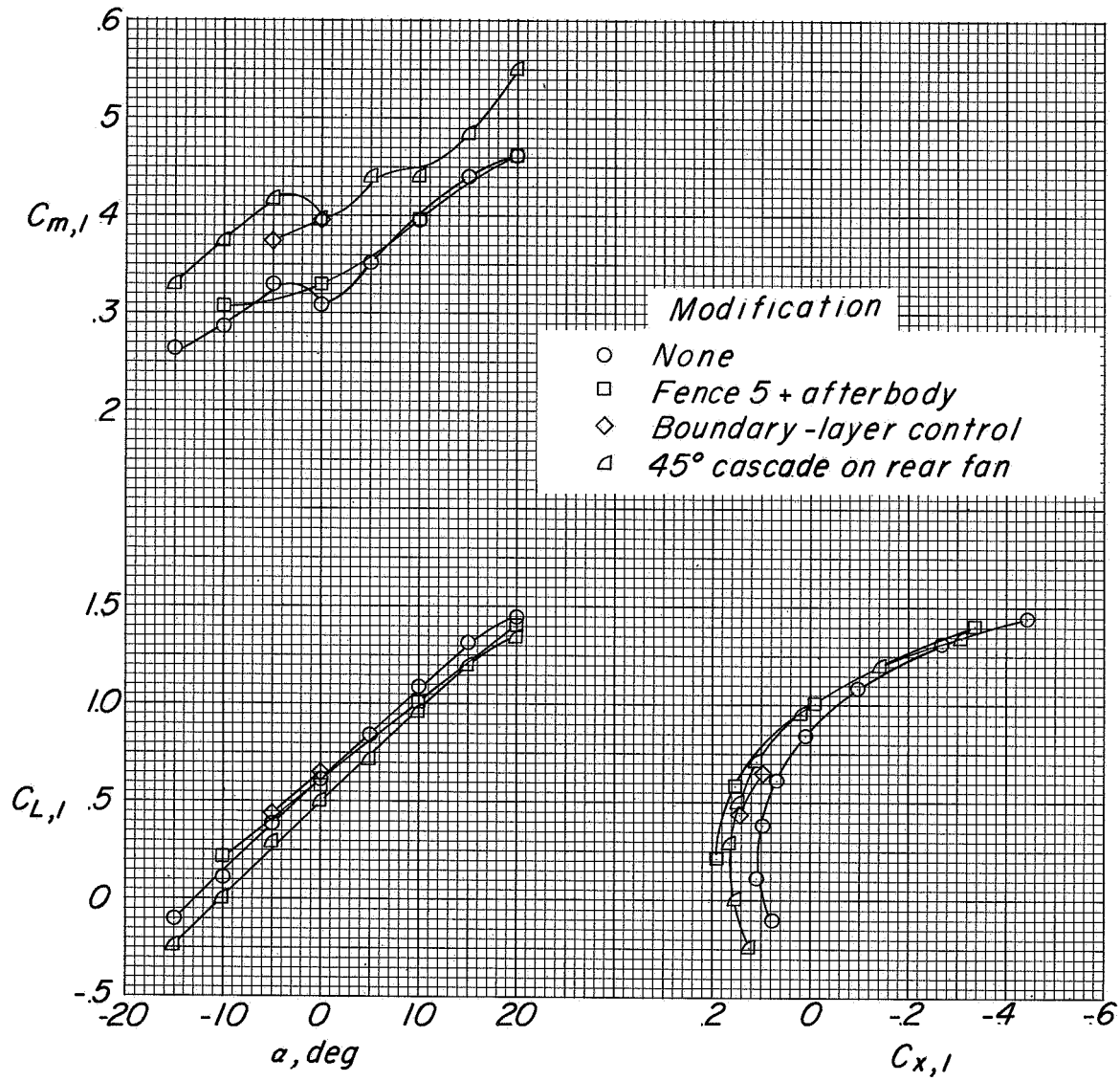
~~CONFIDENTIAL~~



(b) Longitudinal forces and moments.

Figure 18.- Concluded.

~~CONFIDENTIAL~~

~~CONFIDENTIAL~~

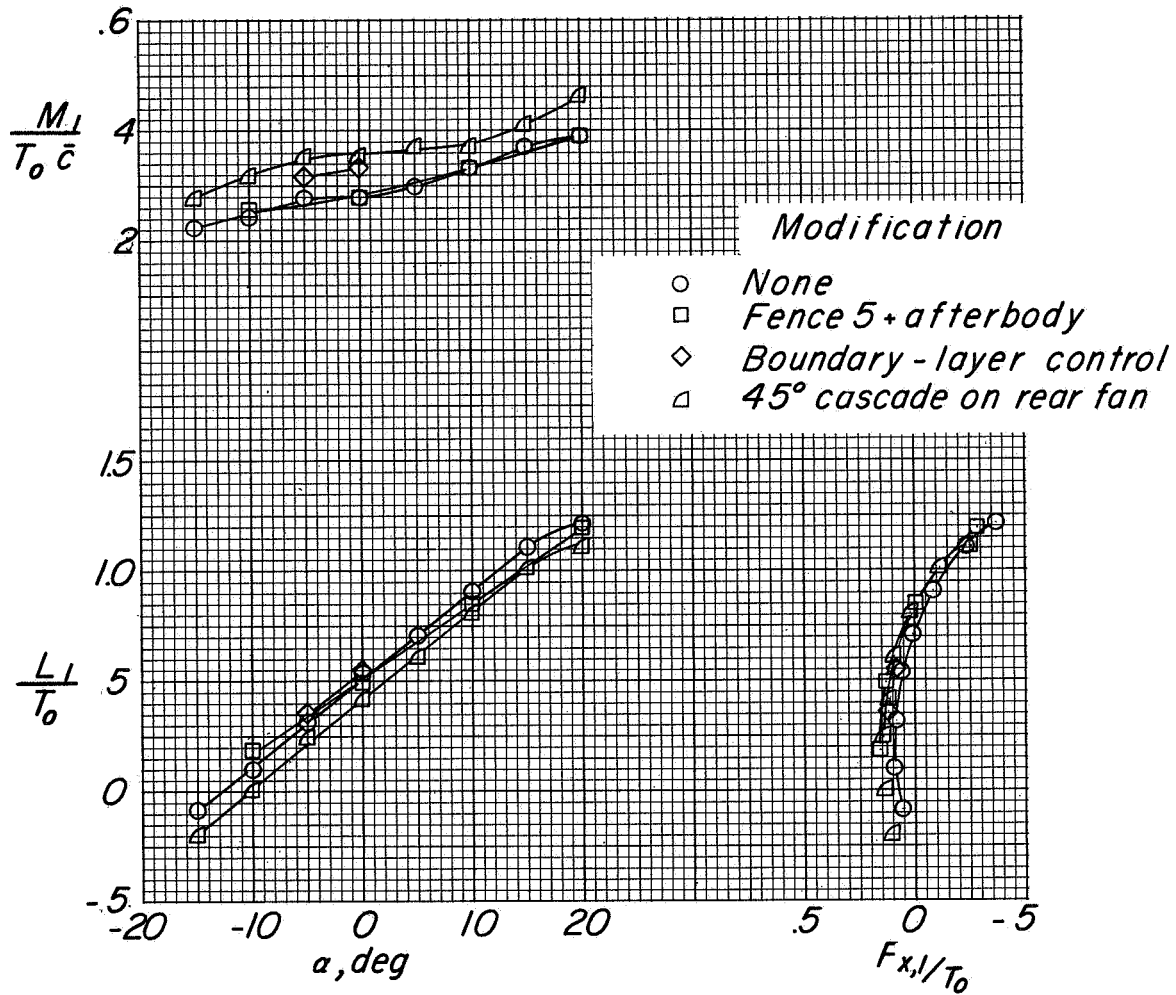
(a) Longitudinal coefficients.

Figure 19.- Effect of various lower-surface modifications on aerodynamic characteristics. $V_\infty/V_j = 0.316$; $\delta = 60^\circ$.

~~CONFIDENTIAL~~

~~CONFIDENTIAL~~

L-1748



(b) Longitudinal forces and moments.

Figure 19.- Concluded.

~~CONFIDENTIAL~~

CONFIDENTIAL

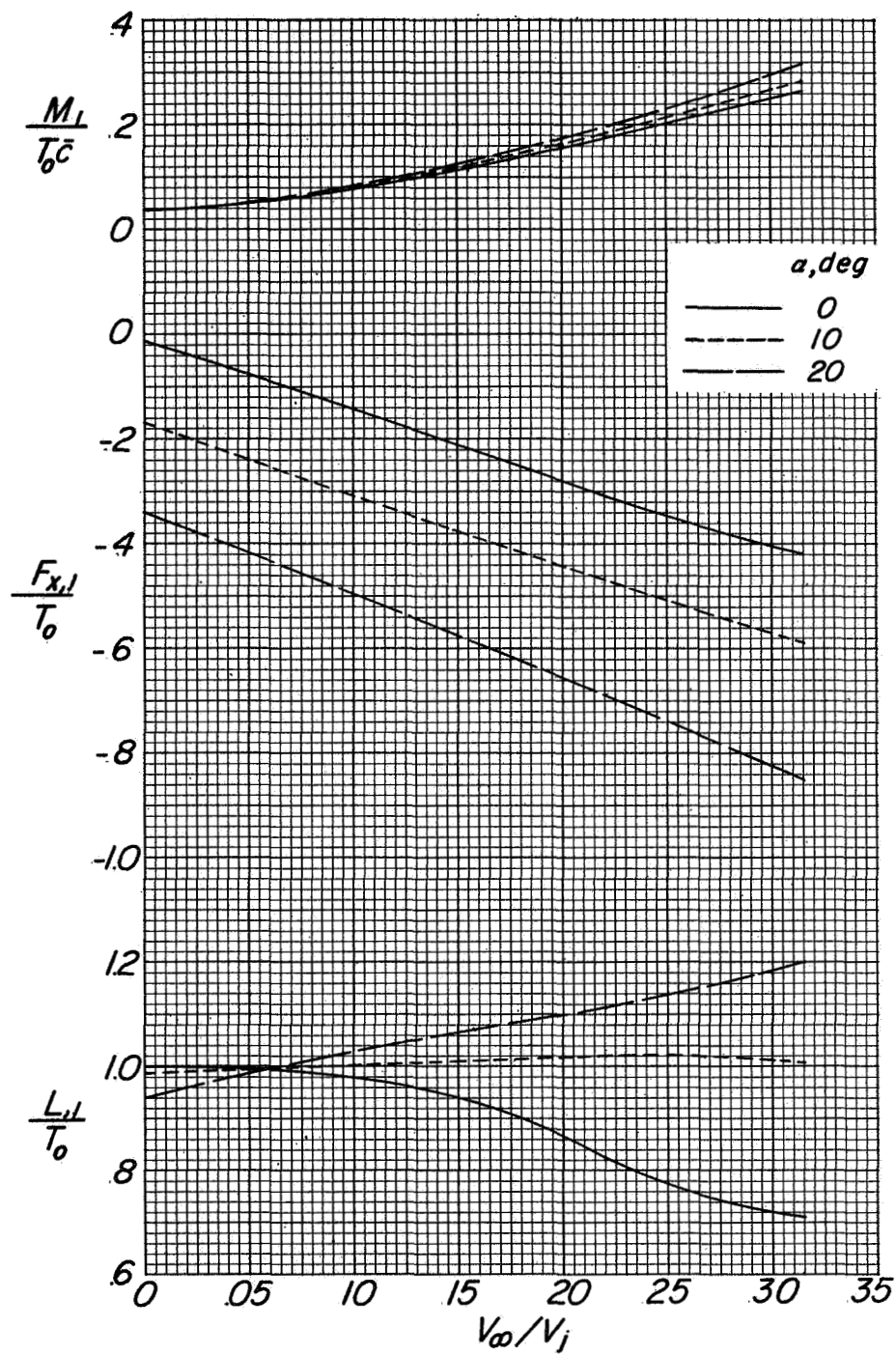
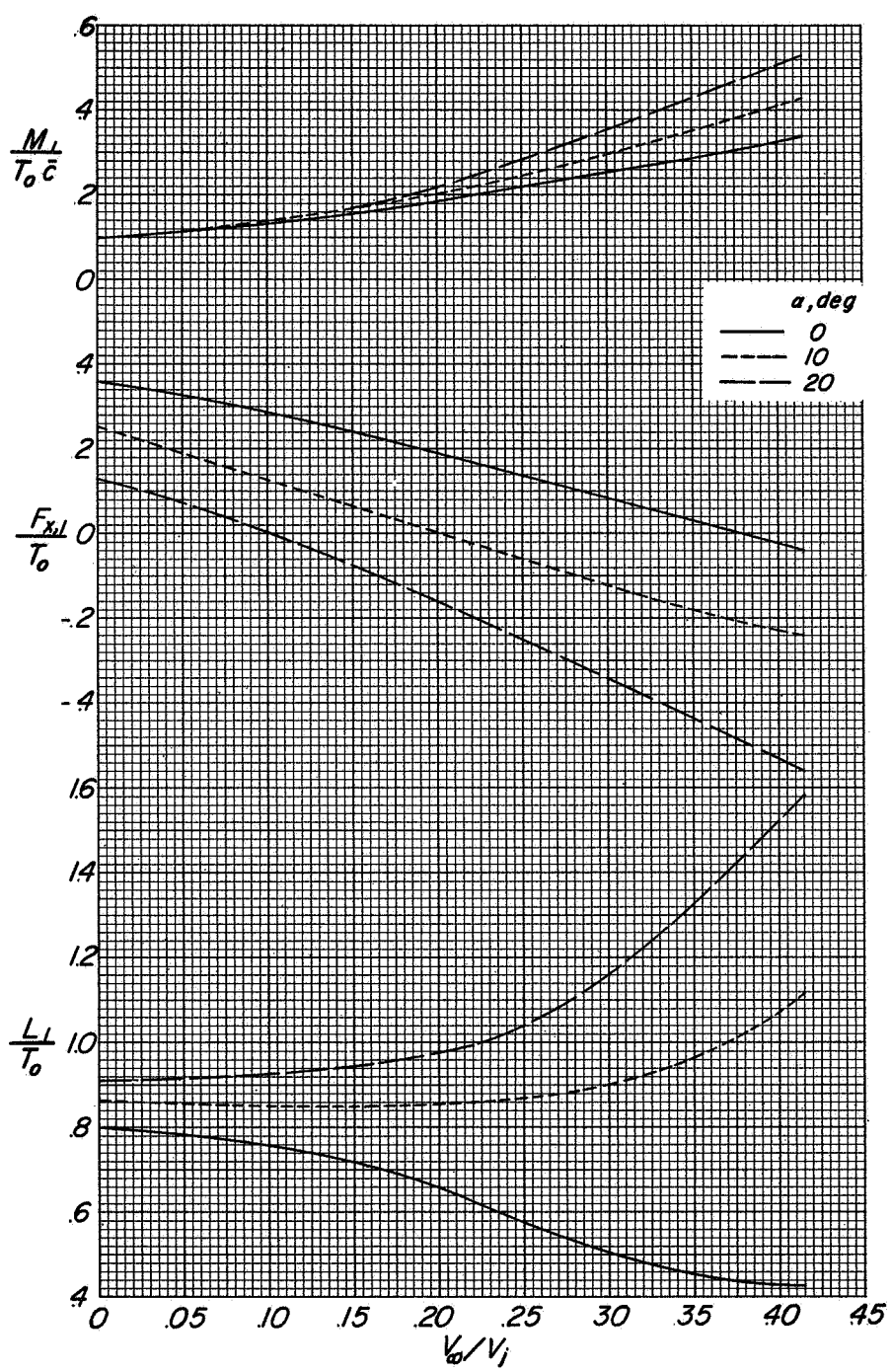
(a) $\delta = 90^\circ$.

Figure 20.- Summary of aerodynamic characteristics.

CONFIDENTIAL

CONFIDENTIAL

L-1748



(b) $\delta = 60^\circ$.

Figure 20.- Concluded.

CONFIDENTIAL

CONFIDENTIAL

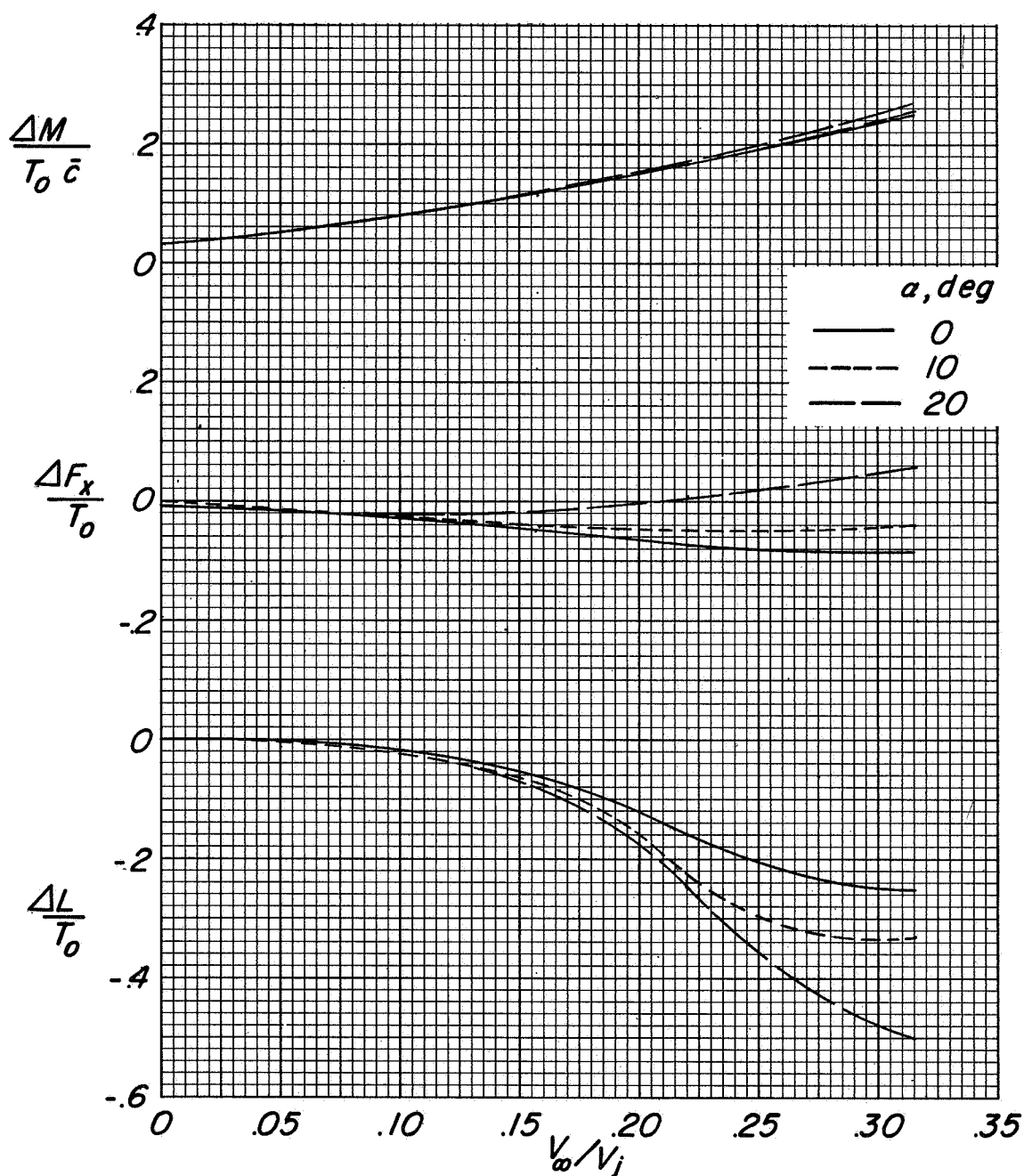
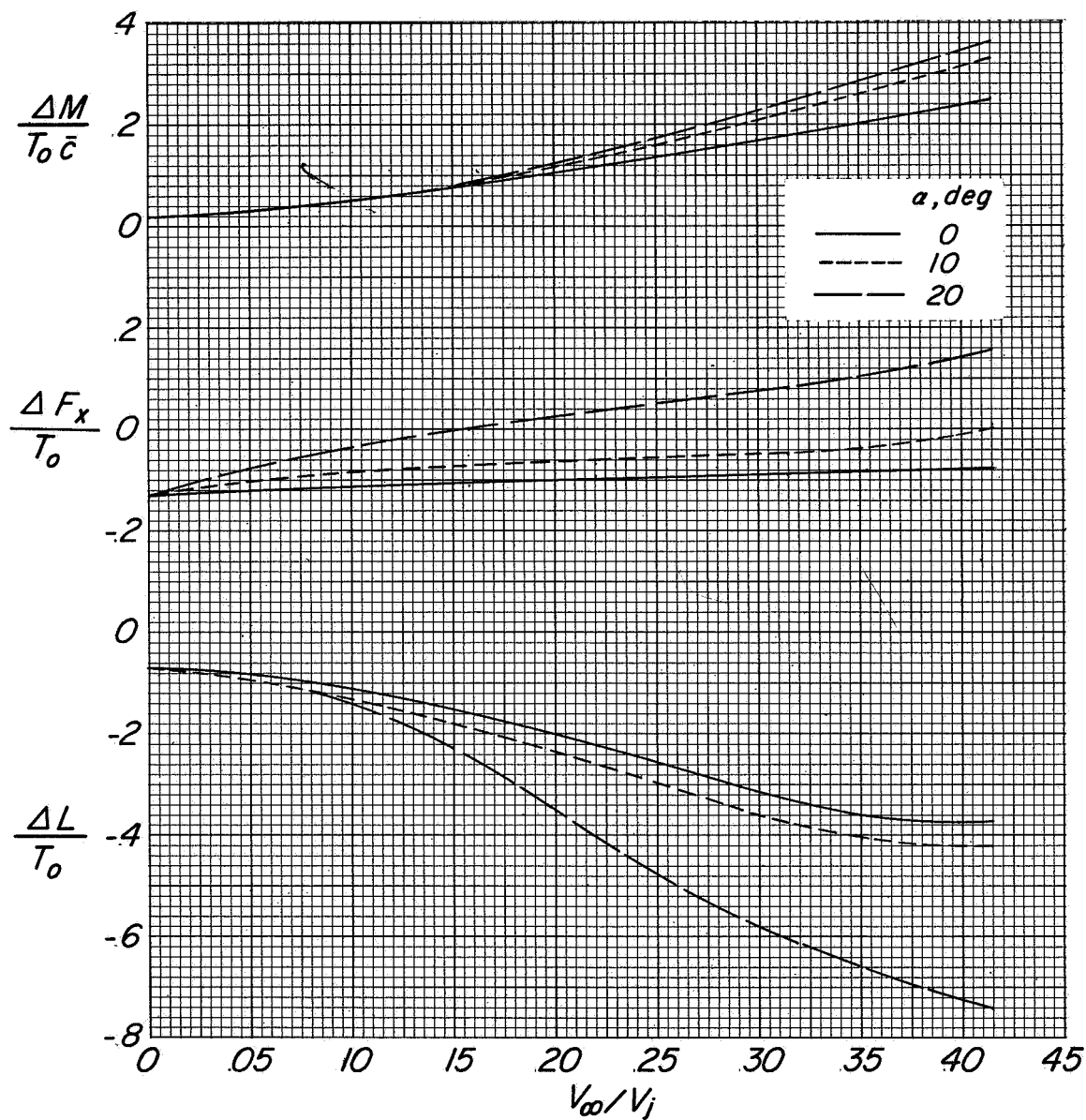
(a) $\delta = 90^\circ$.

Figure 21.- Increments in lift, longitudinal force, and pitching moment due to jet interference.

CONFIDENTIAL

~~CONFIDENTIAL~~

45



(b) $\delta = 60^\circ$.

Figure 21.- Concluded.

~~CONFIDENTIAL~~